Expression, sorting, and segregation of Golgi proteins during germ cell differentiation in the testis

Catherine E. Au[a,b,*], Louis Hermo[a,*], Elliot Byrne[a,b], Jeffrey Smirle[a,b], Ali Fazel[a,b], Paul H. G. Simon[a,b], Robert E. Kearney[c], Pamela H. Cameron[a,b], Charles E. Smith[a], Hojatollah Vali[a], Julia Fernandez-Rodriguez[d], Kewei Ma[b], Tommy Nilsson[a,b], and John J. M. Bergeron[a,b]

[a]Department of Anatomy and Cell Biology, McGill University, Montreal, QC H3A 0C7, Canada; [b]Division of Endocrinology and Metabolism, McGill University Health Centre Research Institute, Montreal, QC H3A 1A1, Canada; [c]Department of Biomedical Engineering Department, McGill University, Montreal, QC H3A 2B4, Canada; [d]Centre for Cellular Imaging, Sahlgrenska Academy, University of Gothenburg, 405 30 Gothenburg, Sweden

ABSTRACT **The molecular basis of changes in structure, cellular location, and function of the Golgi apparatus during male germ cell differentiation is unknown. To deduce cognate Golgi proteins, we isolated germ cell Golgi fractions, and 1318 proteins were characterized, with 20 localized in situ. The most abundant protein, GL54D of unknown function, is characterized as a germ cell–specific Golgi-localized type II integral membrane glycoprotein. TM9SF3, also of unknown function, was revealed to be a universal Golgi marker for both somatic and germ cells. During acrosome formation, several Golgi proteins (GBF1, GPP34, GRASP55) localize to both the acrosome and Golgi, while GL54D, TM9SF3, and the Golgi trafficking protein TMED7/p27 are segregated from the acrosome. After acrosome formation, GL54D, TM9SF3, TMED4/p25, and TMED7/p27 continue to mark Golgi identity as it migrates away from the acrosome, while the others (GBF1, GPP34, GRASP55) remain in the acrosome and are progressively lost in later steps of differentiation. Cytoplasmic HSP70.2 and the endoplasmic reticulum luminal protein-folding enzyme PDILT are also Golgi recruited but only during acrosome formation. This resource identifies abundant Golgi proteins that are expressed differentially during mitosis, meiosis, and postacrosome Golgi migration, including the last step of differentiation.**

Monitoring Editor
Yukiko Yamashita
University of Michigan

Received: Dec 19, 2014
Revised: Feb 27, 2015
Accepted: Mar 19, 2015

INTRODUCTION

The structure, function, biogenesis of the Golgi apparatus, and mechanism of transport of proteins therein remain controversial (Farquhar and Palade, 1998; Gilchrist *et al.*, 2006; Lavieu *et al.*, 2013; Rizzo *et al.*, 2013). A developmental system whereby Golgi protein expression is linked to differentiation-specific changes in the Golgi apparatus structure and function may provide a model to address major controversies (Emr *et al.*, 2009; Klumperman, 2011). Germ cell differentiation in the testis, defined as spermatogenesis, is such a developmental system. Here changes in size, shape, and fate of the Golgi apparatus during cell differentiation are coincident

This article was published online ahead of print in MBoC in Press (http://www.molbiolcell.org/cgi/doi/10.1091/mbc.E14-12-1632) on March 25, 2015.

*Joint first authors.

Author contributions: C.E.A. and L.H.: proteomics, subcellular fractionation, imaging, and writing of the paper; A.F.: subcellular fractionation and electron microscopy; R.E.K.: bioinformatics; P.H.C.: biochemistry of GL54D; E.B., J.S., C.E.S., H.V., J.F.-R., P.H.G.S., K.M., and T.N.: imaging; J.J.M.B.: supervised all aspects and wrote the paper with L.H. and C.E.A.

Address correspondence to: John J. M. Bergeron (john.bergeron@mcgill.ca).

Abbreviations used: A, acrosome; CL, cytoplasmic lobe; E, epididymal epithelium; EM, electron microscopy; EndoH, endoglycosidase H; ER, endoplasmic reticulum; G, Golgi apparatus; GFP, green fluorescent protein; GL54D, glycosyltransferase 54 domain-containing protein; GNT1IP, GlcNAcT-I inhibitory protein; IS, initial segment; IF, immunofluorescence; IHC, immunocytochemistry; Ley, Leydig cells; LM, light microscopy; MS, mass spectrometry; Neur + O-Glyco, neuraminidase plus *O*-glycosidase; P, pachytene spermatocytes; PBS, phosphate-buffered saline; PBS-G, PBS containing 0.2% fish skin gelatin; PL, preleptotene spermatocytes; PMSF, phenylmethylsulfonyl fluoride; PNGase F, peptide *N*-glycosidase F; RBs, residual bodies; RS, round spermatids; S, Sertoli cells; SE, seminiferous epithelium; TBS, Tris-buffered saline; TG, testis Golgi; TM9, transmembrane 9 superfamily.

with changes in Golgi function (Hermo *et al.*, 2010a). Detailed electron microscopy (EM) studies have documented Golgi apparatus morphology from mitosis of spermatogonia, when plasma membrane is needed for new daughter cells, to the meiotic divisions of spermatocytes, when the Golgi apparatus undergoes a dramatic enlargement in size before its breakdown and distribution to each of the four daughter cells formed during the second meiotic division (Suarez-Quian *et al.*, 1991; Thorne-Tjomsland *et al.*, 1991). Equally detailed EM descriptions have defined the morphology of the Golgi apparatus during the 19 steps of spermatid development (spermiogenesis). This includes early spermiogenesis (step 1–7 spermatids), when the Golgi apparatus takes on a hemispherical shape, whereupon it elaborates the acrosome (Griffiths *et al.*, 1981; Hermo *et al.*, 2010a), a lysosome-like structure capping the nucleus and required for eventual sperm fertilization. From steps 8 to 15 of spermiogenesis, EM has also defined the morphology of the spherical Golgi apparatus as it migrates away from the acrosome but remains involved in glycoprotein modifications (Clermont and Tang, 1985; Batista *et al.*, 2012). Oko *et al.* (1993) proposed that thereafter, in differentiation, the individual flattened cisternae of the Golgi stack separate from each other as the Golgi apparatus undergoes fragmentation (Susi *et al.*, 1971), with segregation of these components within a cytoplasmic bulge at the neck or connecting piece of the flagellum in step 19 spermatids, known as the forming cytoplasmic droplet. The latter is retained by sperm as they mature in the epididymal duct (Hermo *et al.*, 2010b). Its characterization and proposed function has been resolved through proteomics, and the structure has been renamed the Hermes body.

In this study, we explore the Golgi protein makeup of germ cells to assess whether their expression coincides with the major structural modifications and functions of the Golgi apparatus during their differentiation and with Golgi proteins retained in the Hermes body. A methodology designed to isolate the Golgi apparatus of germ cells from whole adult rat testis homogenates reveals 1318 proteins characterized quantitatively. Twenty of these are localized by light microscopy (LM) immunocytochemistry (IHC) and seven by immunofluorescence (IF) in each of the more than 64 different recognizable cell types undergoing germ cell differentiation during the 14 stages of the spermatogenic cycle and the eventual appearance in the Hermes body. For the seminiferous epithelium, such mapping is straightforward, as it is based on the well-accepted classification system of Leblond and Clermont (1952).

This resource describes the first attempt to link Golgi apparatus protein expression with changes in Golgi apparatus structure, location, and function during germ cell differentiation. Highly abundant and previously unknown Golgi proteins are uncovered. A segregation of Golgi proteins during acrosome formation provides insight into Golgi identity and its role in acrosome biogenesis. The distribution of Golgi proteins is uncovered for mitosis, meiosis, acrosome formation, and postacrosomal germ cell differentiation. As well, an unexpected selective expression of Golgi proteins is found in the last step of germ cell differentiation, that is, step 19 spermatids.

RESULTS

A Golgi fraction from whole adult rat testis homogenates corresponds to spermatocyte/spermatid Golgi

The spherical compact Golgi apparatuses characteristic of germ cells were isolated from whole testis homogenates as described in *Materials and Methods*. By random EM sampling of isolated Golgi fractions displayed on filters, the Golgi apparatus is shown to be large, compact, spherical in shape, and formed of stacks composed of numerous flattened cisternae and associated vesicles (Figure 1A). These features (Figure 1B) correspond to those of spermatocyte and spermatid Golgi (Hermo *et al.*, 1979, 1980; Thorne-Tjomsland *et al.*, 1988) but not to the Golgi apparatus of Sertoli and Leydig cells (Christensen, 1975; Hermo *et al.*, 1980; Rambourg *et al.*, 1979). By morphometry ($n = 4$ isolates), 51.6% ± 13.3% of the membranous structures were scored as intact, compact, stacked Golgi apparatuses. Tomography of thick sections of the isolated testis Golgi (TG) fractions reveal the sheet-like appearance of the flattened cisternae (Figure 1C and Supplemental Movie 1).

Characterization of the proteins of the TG fractions was done as described previously (Gilchrist *et al.*, 2006), with protein abundances estimated from spectral counting (redundant peptides). Proteins characterized in the TG fractions were compared with a subcellular fraction, the Hermes body, isolated from epididymal sperm (Au *et al.*, 2015) and from liver-derived organelles of the early secretory pathway (Gilchrist *et al.*, 2006). Using the same strategy as Gilchrist *et al.* (2006), we subdivided proteins into 22 functional categories and mapped their codistributions in all samples characterized (Au *et al.*, 2015). Proteins were also sorted by their order of abundance in the isolated TG fraction (Supplemental Table S1).

The most abundant protein, GL54D, is a male germ cell–specific Golgi-resident protein

Unexpectedly, the most abundant protein of the isolated TG fractions (Supplemental Table S1) was a protein of unknown function previously unreported as a protein. Annotated by UniProtKB/Swiss-Prot as glycosyltransferase 54 domain-containing protein (GL54D), it was undetectable in liver subcellular or isolated Hermes body fractions (Figure 1D). Tryptic peptides covering the sequence of the GL54D protein were characterized, and antibodies were raised to a peptide sequence (Figure 1E, see legend).

Western blots of TG fractions using this antibody revealed a major band at 61 kDa (Figure 1F). Triton X-114 partitioning into the detergent phase identified the protein as an integral membrane protein. The protein mobility on SDS–PAGE is unaffected by endoglycosidase H (EndoH) digestion but sensitive to peptide *N*-glycosidase F (PNGase F). This increased the mobility of the protein to an estimated molecular weight of 49 kDa, corresponding to the predicted mass of the unglycosylated protein in Swiss-Prot. A reproducibly small shift of increased mobility was found after neuraminidase plus *O*-glycosidase (Neur + O-Glyco) treatment due to neuraminidase cleavage of terminal sialic acid residues (Figure 1F).

With the same peptide-specific antibody, localization in sections of adult rat testes reveals immunoreactivity for GL54D exclusively in the Golgi apparatus of germ cells (Figure 1, G–I) indicating that the isolated fraction was germ cell in nature. Specifically, the Golgi apparatus of pachytene spermatocytes beginning at stage VII and extending up to stage XIV are immunoreactive. GL54D immunoreactivity in the Golgi apparatus of spermatocytes undergoing meiotic divisions at stage XIV of the cycle shows several small discrete reactive bodies destined for the daughter cells (Figure 1J) and the maintenance of Golgi identity during meiotic divisions (Suarez-Quian *et al.*, 1991). The Golgi apparatus of spermatids is immunoreactive at steps 1–15 of spermiogenesis, (Figure 1G). In step 16 spermatids, immunoreactivity is detected in several small discrete spherical structures, corresponding to dispersed Golgi components (Figure 1H). In step 17–18 spermatids, GL54D is undetectable (Figure 1I), and this is also the case for the forming Hermes body in step 19 spermatids and in epithelial cells and sperm in the epididymis (unpublished data).

The chronological expression of GL54D as assessed for all 63 morphologically distinct germ cells during spermatogenesis is

highlighted in blue in Figure 2A, corresponding to a duration of more than 3 wk (Clermont, 1972).

An exact coincidence of onset of expression of GL54D is found with that of the glucose transporter 3 (GLUT-3), a plasma membrane protein decorating germ cells (highlighted in red in Figure 2A), with both proteins being only expressed in germ cells of the testis. Examples of GLUT-3 expression at different stages of the cycle of germ cell differentiation are shown in Figure 2, B–D.

We tested whether GL54D could be tagged and targeted to the Golgi apparatus of somatic cells, where it is not normally expressed. Heterologous expression of the green fluorescent protein (GFP)-tagged protein in HepG2 cells revealed a Golgi apparatus localization confirmed by colocalization with galactosyl transferase antibody (Figure 3, A–C). GL54D (Figure 3D) also colocalized with the endogenous type II integral membrane protein ERMAN1 (Figure 3, E–G), which is also known to be Golgi localized (Pan *et al.*, 2013; Smirle *et al.*, 2013), and the type I integral membrane protein TMED7/p27 (Figure 3, F–G). GL54D-GFP localization is reversibly dependent on brefeldin A, as expected for a Golgi-targeted resident protein (Figure 3, H and I).

TM9SF3 is a new abundant Golgi marker for somatic and germ cells

To test whether any proteins of unknown function of the TG fractions are common to the Golgi apparatus of somatic cells, we assessed the proteomics data of Figure 1D for those proteins enriched in both testis and liver Golgi fractions but depleted from liver endoplasmic reticulum (ER) fractions. Three TM9 (transmembrane 9 superfamily) proteins of unknown function (Figure 1D) satisfy these criteria. The proteins are all enriched in Golgi-derived COPI (coatomer protein complex I) vesicles, as deduced for other Golgi-resident proteins (Gilchrist *et al.*, 2006). Testing of the prediction reveals TM9SF3 localization to the Golgi apparatus of germ and somatic cells (Figure 4, A–D), including Sertoli and Leydig cells (Figure 4, B–D). In germ cells, immunoreactivity extends from spermatogonia up to step 15 spermatids (Figure 4, A and B). During meiosis, prominent immunoreactivity in several small discrete Golgi bodies of spermatocytes undergoing their meiotic divisions is seen (Figure 4E). In step 16 spermatids, smaller dispersed elements corresponding to dispersed Golgi components (Oko *et al.*, 1993) are immunoreactive (Figure 4C), but protein expression is undetectable during later steps of differentiation (i.e., step 17–19 spermatids, Figure 4D) or later still in the Hermes body of epididymal sperm (Figure 4F). The strong Golgi localization to somatic epithelial cells of the epididymis (Figure 4F) serves as an internal control to indicate the cell differentiation specificity of TM9SF3 expression and localization to germ and somatic cells. The differential expression of GL54D and TM9SF3 is summarized in Figure 5 in the context of other Golgi-localized proteins characterized in this study. Thus the subcellular fractionation strategy to isolate germ cell Golgi apparatus from whole testis homogenates uncovered two abundant proteins of the TG fraction. These proteins define new Golgi markers, with GL54D being germ cell specific and TM9SF3 and other TM9 family members likely being common to the Golgi apparatus of germ and somatic cells.

Glycosyl modification enzymes are abundant as expected for their role in male fertility

Complex sugar modifications on glycoproteins of germ cells by the Golgi apparatus are essential for germ cell differentiation (Fukuda and Akama, 2002; Batista *et al.*, 2012). The cognate Golgi glycan-modifying enzymes are well represented in isolated TG fractions (Figure 6A). Hierarchical clustering reveals abundant testis-specific glycan-modifying proteins as characterized in separate isolates of liver ER, Golgi, COPI vesicles, testis germ cell Golgi, and Hermes body epididymal subcellular fractions.

The germ cell–specific glycan-modifying enzyme MANIIX (Igdoura *et al.*, 1999) is the most abundant. Well-characterized antibodies localize the protein to the Golgi apparatus of step 1–7 spermatids during acrosome formation. The strongest immunoreactivity, however, is in step 15–19 spermatids, when the Golgi apparatus or a portion of it is observed as a spherical entity (Figure 6, B and C). In the step 19 spermatids, MANIIX immunoreactivity preferentially localizes to Golgi remnants in residual bodies with some diffuse reaction in the forming Hermes body in step 19 spermatids (Figure 6D) and in epididymal sperm (Supplemental Figure 1A).

The more ubiquitous housekeeping MAN2α1 is of lower abundance in TG fractions, although highly abundant in liver Golgi and Golgi-derived COPI vesicles, and, as expected, the protein is of low to undetectable abundance in ER fractions (Figure 6A). In testis, MAN2α1 localizes to the Golgi/developing acrosome of step 1–7 spermatids and Sertoli cells (Figure 5E), confirming published work (Ramalho-Santos *et al.*, 2001). While absent from steps 8 to 18, expression returns in the forming Hermes body at step 19 (unpublished data). Like MANIIX, MAN2α1 also localizes to epididymal sperm (Supplemental Figure 1B). GlcNAc transferase 1, as expected from transcriptional profiling (Chalmel *et al.*, 2007), is undetectable in the TG fraction (Supplemental Table S1) but readily characterized in liver Golgi fractions (Gilchrist *et al.*, 2006). The distribution profiles of these glycan-modifying enzymes is shown in Figure 5 to illustrate their differential expression. The germ cell–specific glycosyl modification enzymes further substantiate the isolated TG fraction as germ cell Golgi derived.

Differential expression of tethering, GTP binding, and membrane traffic regulatory proteins

Vesicle-tethering proteins specify the sorting of incoming membrane traffic to the Golgi apparatus (Wong and Munro, 2014). The most abundant of these proteins are shown in Figure 6F in order of their abundances in the TG fraction. These include giantin and golgin 97 (Figure 6F), previously localized to the Golgi apparatus of germ cells (Moreno *et al.*, 2000a,b; Ramalho-Santos *et al.*, 2001). The TATA element regulatory factor 1 (also known as TMF/ARA160) is also abundant and, despite its name, is a known Golgi-resident protein (Lerer-Goldshtein *et al.*, 2010; Miller *et al.*, 2013; Yamane *et al.*, 2007). Also abundant are Golgi SNAREs (soluble NSF [*N*-ethylmaleimide-sensitive fusion protein] attachment protein receptors), AAA proteins (NSF, P97), and annexin A6.

GRASP55 and GPP34 (also known as Golph3), examples of proteins in this category, both localize to the Golgi apparatus of step 1–7 spermatids and the developing acrosome (Figure 6, G and H). GRASP 55 is undetectable in germ cells later in differentiation, whereas GPP34 expression returns in the forming Hermes body in step 19 spermatids (Supplemental Figure 1C) and is maintained in epididymal sperm (Supplemental Figure 1D).

GBF1, assigned to the GTPase category (Figure 6I), is prominent in the Golgi apparatus of spermatocytes and early spermatids from step 1–7 spermatids, including the acrosome (Figure 6J), the forming Hermes body in step 19 spermatids (Supplemental Figure 1E), and epididymal sperm (Supplemental Figure 1F). The differential expression of these proteins is depicted in Figure 5 for comparison.

Other abundant GTPases—Rabs 1, 2, and 6 (Figure 6I)—identified by proteomics are all known Golgi Rabs (Gilchrist *et al.*, 2006), with some previously identified in germ cells (Ramalho-Santos *et al.*, 2001).

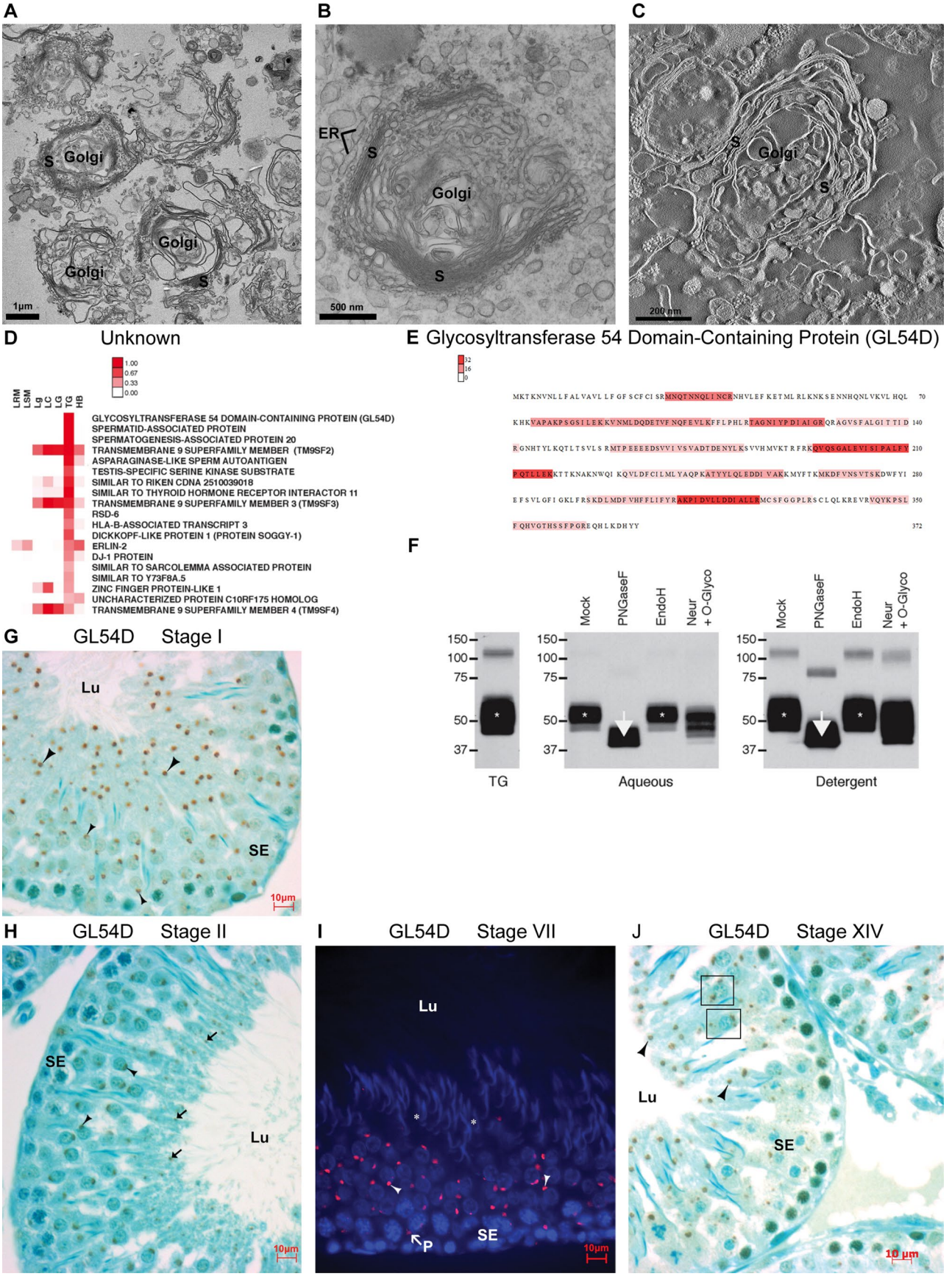

FIGURE 1: TG fractions correspond to the germ cell Golgi apparatus with GL54D an exclusive marker for the germ cell Golgi apparatus. (A and B) EM of isolated TG fraction (A) and step 12 spermatid Golgi (B) show similar features. (C) Tomography of Golgi stacks (S) of TG fraction. (D) Heat map of 19 proteins of unknown category sorted by

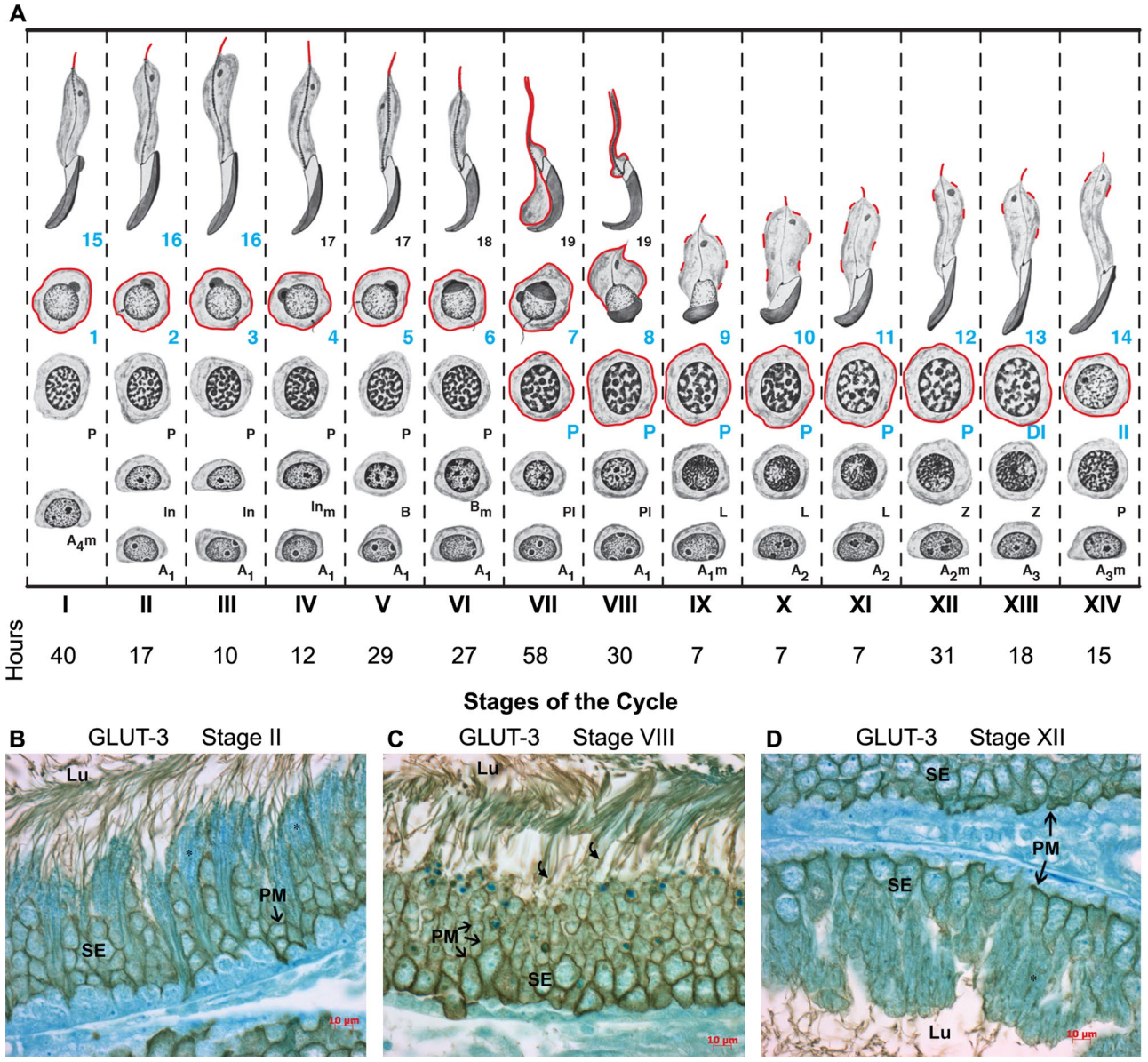

FIGURE 2: Onset of GLUT-3 expression coincides with GL54D in germ cell differentiation. (A) The 64 different cell types undergoing germ cell differentiation are organized into 14 stages of the spermatogenic cycle with their duration in hours (modified from Dym and Clermont, 1970). Expression of GLUT-3 is indicated in red. The cells expressing GL54D are indicated in blue (from P to 16). (B–D) Immunoreactivity of GL54D in stages II, VIII, and XII. Plasma membrane (PM) immunoreactivity is clearly observed but with cell differentiation specificity. Cells that show no immunoreactivity are indicated with asterisks in B; spotty immunoreactivity seen in cells in D is also indicated with an asterisk.

TMED family members are Golgi markers of germ cell morphogenesis and the Hermes body

Classified in the Traffic category, the Golgi TMED/p24 family proteins are highly abundant, with five different TMED members characterized in the TG fraction (Figure 7A). These include TMED2, TMED4, TMED7, TMED9, and TMED10. TMED7/p27 is of nearly equal abundance in the Hermes body and TG fractions. It localizes to the spherical Golgi apparatus of all germ cells up to step 15 spermatids (Figure 7, B–E). At the later steps 17–19 (Figure 7E), smaller reactive sites are found with reaction maintained in the forming Hermes body in step 19 spermatids (Figure 7F) and in epididymal sperm (Au *et al.*, 2015).

TMED4/p25 expression (Figure 7G) localizes to Golgi apparatus of spermatocytes and late spermatids, similar to TMED7/p27. However,

abundance in TG fractions. (E) Primary sequence of rat GL54D with deduced peptide sequences represented (heat map with scale bar). Monospecific polyclonal antibodies were raised to a synthetic peptide from aa 355–372. (F) Western blots of GL54D. Left, TG fraction (TG); center, aqueous extract after Triton X-114 phase partitioning; right, detergent phase. Digestions with no enzyme (Mock), PNGase F, EndoH, and Neur + O-Glyco. Asterisk indicates GL54D; arrow indicates 12-kDa shift. (G and H) IHC and (I) IF of GL54D in germ cell Golgi apparatus of spermatocytes and spermatids. Arrows indicate fragmenting Golgi apparatus of late spermatids. (J) Golgi bodies (boxes) retain Golgi identity with GL54D immunoreactivity during meiotic divisions of spermatocytes.

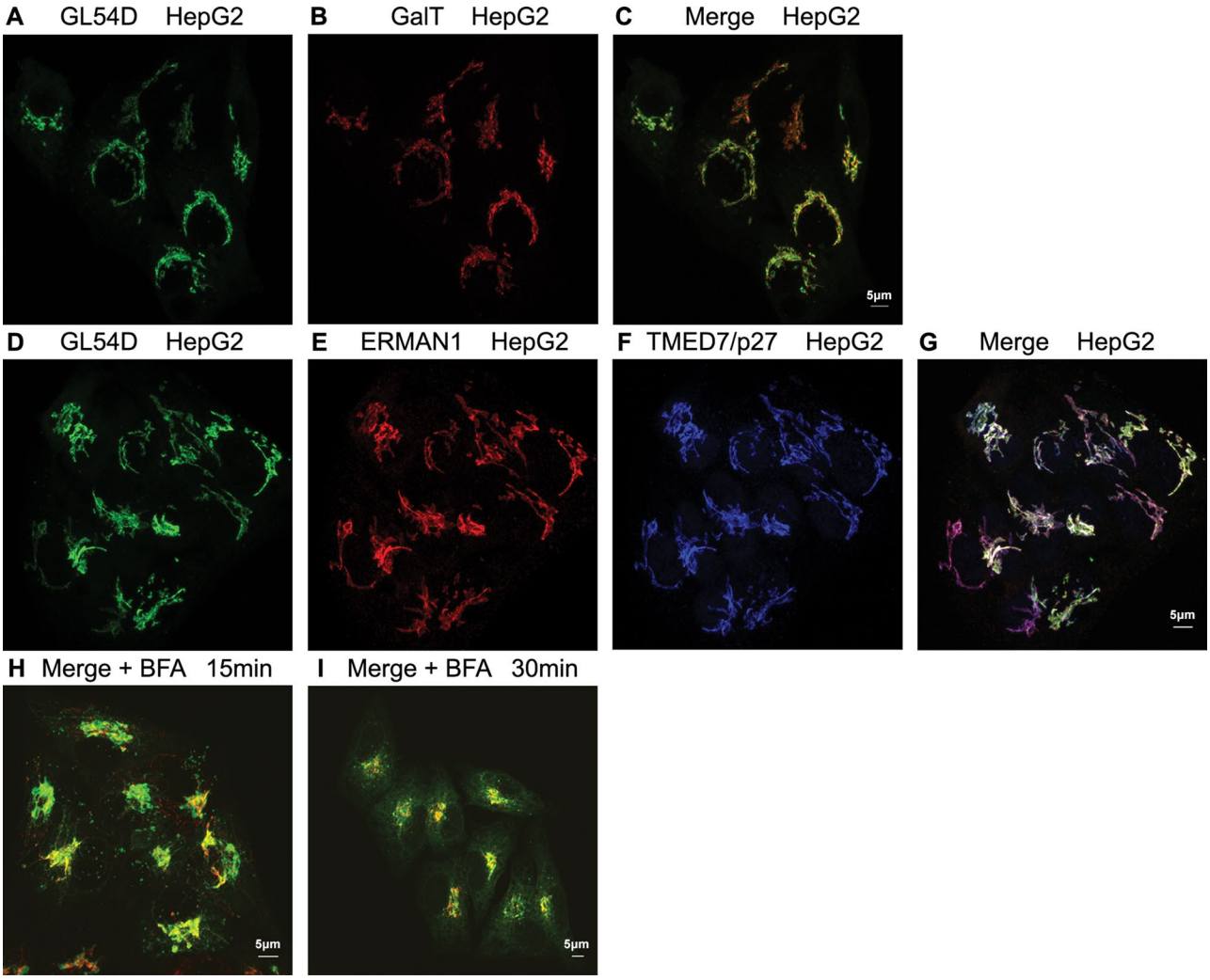

FIGURE 3: Expression alone targets GL54D to the Golgi apparatus in HepG2 cells. (A) Confocal IF of GL54D-GFP stably transfected HepG2 cells, (B) after immunostaining with monoclonal anti-galactosyltransferase and (C) colocalized (merged). (D–G) Comparison of GL54D-GFP (D) with monoclonal anti-ERMAN1 (E) and polyclonal anti-TMED7/p27 (F) and colocalized (G, merged). Confocal merge of GL54D and anti-galactosyl transferase after brefeldin A (BFA) for (H) 15 min or (I) 30 min.

immunoreactivity is undetected in step 17–19 spermatids and epididymal sperm (Supplemental Figure 2A). Remarkably, expression of TMED2/p24 is exclusive to the forming Hermes body in step 19 spermatids (Figure 7H) and epididymal sperm (Supplemental Figure 2B). Such replacement of different TMEDs during differentiation is now well accepted, reflecting their different cargo specificities (Strating and Martens, 2009). These distributions are summarized in Figure 5.

In the Traffic category (Figure 7A), the Golgi lectin VIP36 (Reiterer *et al.*, 2010) is prominent, as are SNX5 and VPS35, known proteins of the endocytic arm of membrane trafficking (Bonifacino and Hurley, 2008). Other well-known abundant Golgi trafficking proteins in the TG fractions (Figure 7A) include ERGIC53, KDEL receptor, Golph1, and RER1, whose differential expression during spermatogenesis awaits investigation.

Unexpected Golgi localization of abundant proteins during acrosome formation

The second most abundant protein in the isolated TG fraction is HSP70.2 (Supplemental Table S1). With well-characterized antibodies (Mamelak and Lingwood, 2001), prominent immunoreactivity is seen in the Golgi apparatus and acrosome of step 1–7 spermatids (Figure 8A and inset). This represents the first Golgi localization for this molecular chaperone but only during acrosome formation. The membrane fusion and vesicular-budding protein annexin A6 is also prominent (Figure 8B) with dual Golgi and acrosome localization in step 1–7 spermatids.

Three proteins previously considered as ER restricted (PDILT1, UBXD8, and sapreticulin) are Golgi localized but also only during acrosome formation (Figure 8, C–E). Immediately afterward, PDILT, the testis-specific protein disulfide isomerase, returns to its expected ER location (the immunoreactive cytoplasmic lobes of late spermatids correspond to ER [Figure 8C], as reported by van Lith *et al.*, 2007). UBXD8 (Figure 8D) localizes to the cytoplasm (ER) of pachytene spermatocytes, but is Golgi located only during acrosome formation.

Sapreticulin is a noteworthy luminal ER protein with a saposin B domain previously characterized as a luminal ER protein in liver or when expressed heterologously in HepG2 cells (Gilchrist *et al.*, 2006). In testis, the protein localizes to the Golgi apparatus and the forming acrosome in early spermatids (Figure 8E) and then shifts to the cytoplasm (ER) of late spermatids.

A cargo protein of poorly understood function, FAM3C, is also seen in the Golgi apparatus and acrosome of step 1–7 spermatids

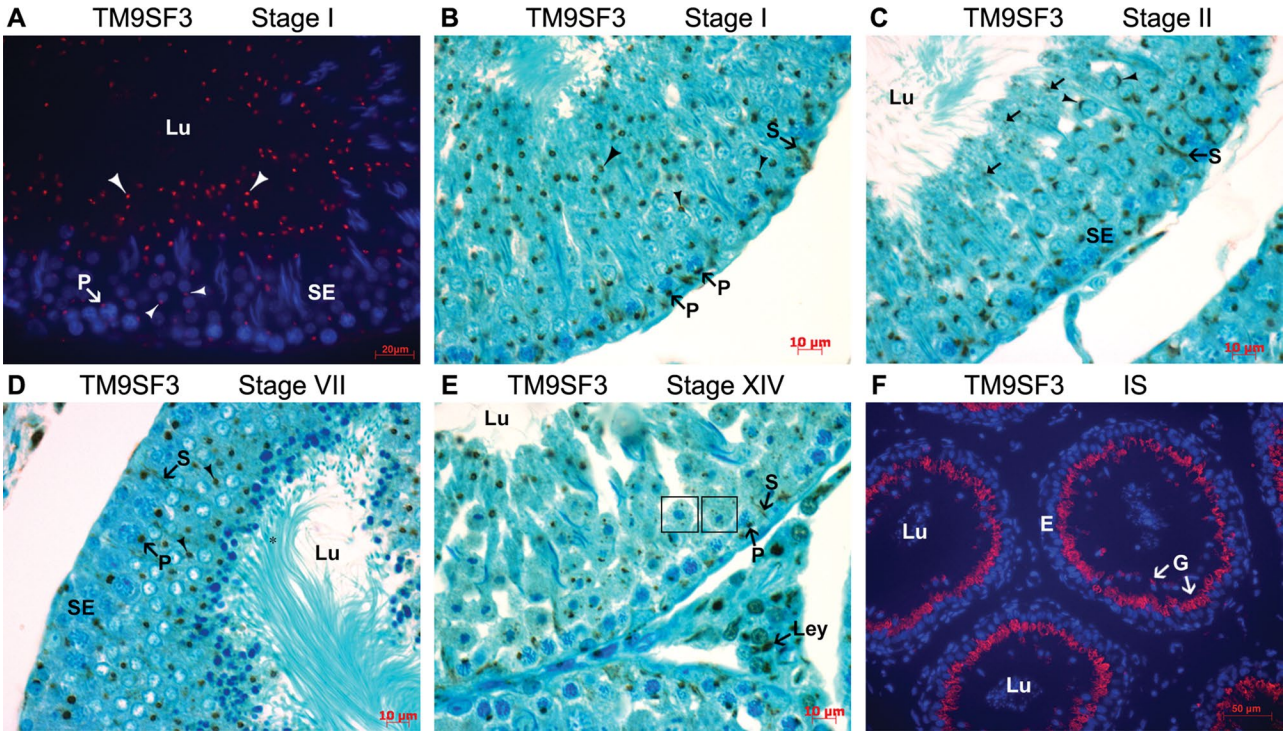

FIGURE 4: TM9SF3 is a Golgi marker for germ and somatic cells. (A) IF and (B–E) IHC of TM9SF3 reveal Golgi immunoreactivity in germ cells, meiotic Golgi bodies (boxes), and Sertoli cells. Arrows indicate fragmenting Golgi apparatus of late spermatids. (F) IF showing reactive Golgi of epithelial epididymal cells but unreactive spermatozoa in lumen.

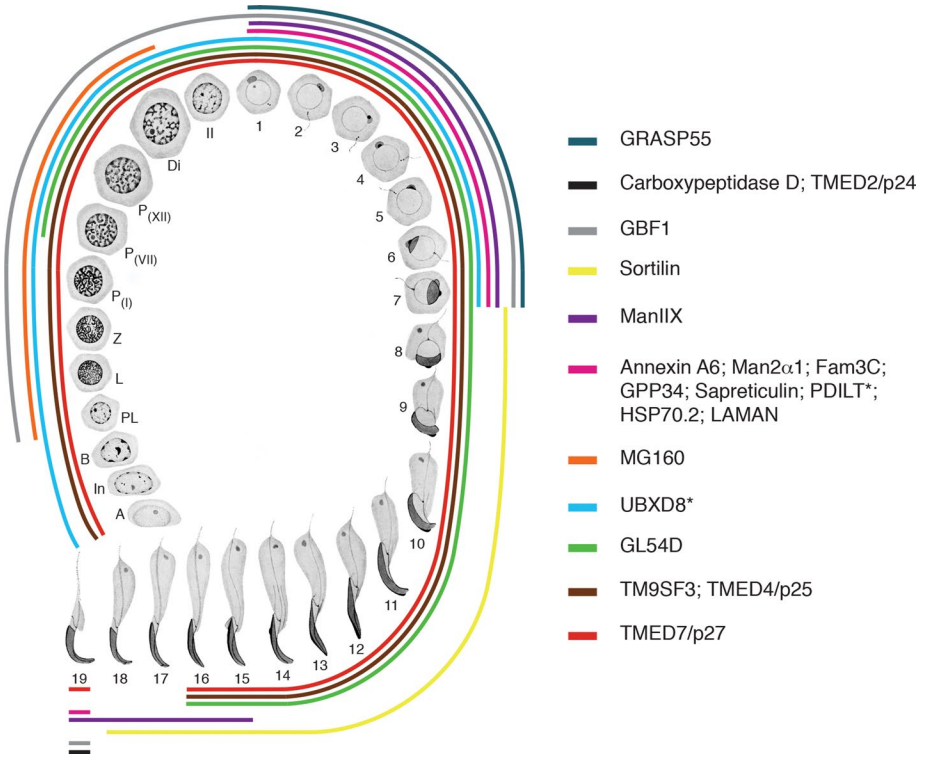

FIGURE 5: Patterns of Golgi-localized protein expression during germ cell differentiation in testis. The expression of GL54D and TM9SF3 is shown in 33 representative cells during spermatogenesis. Also indicated are all Golgi-localized proteins whose expression is mapped during differentiation. Each colored line represents immunoreactivity for Golgi-localized proteins in germ cell differentiation based on maximal expression for each antibody. Spermatogonia: types A, intermediate (In), and B. Primary spermatocytes: preleptotene (PL), leptotene (L), zygotene (Z), pachytene (P), and diplotene (Di); and secondary spermatocytes (II); and steps 1–19 of spermiogenesis (modified from Leblond and Clermont (1952)). PDILT and UBXD8, as indicated by asterisks, are also noted in the ER.

(Figure 8F), as is the lysosomal/acrosomal protein LAMAN (Figure 8G). The isolated TG fraction does not show contamination from acrosomes by EM or acrosomal proteins by proteomics, including LAMAN (Supplemental Table S1). Regardless, the amplification immunohistochemistry method used here successfully revealed its localization in the Golgi apparatus and acrosome (Figure 8G).

Except for UBXD8, all of the above proteins become expressed in the forming Hermes body in step 19 spermatids and epididymal sperm (Supplemental Figure 3, A–D). The differential expression of these proteins is shown in Figure 5 for comparison with other Golgi proteins localized during germ cell differentiation.

The high abundance of the nuclear sorting protein RanBP5 in the isolates (Figure 6I and Supplemental Table S1) is unexplained. Known at the RNA level to be expressed in spermatids (Loveland *et al.*, 2006), there is

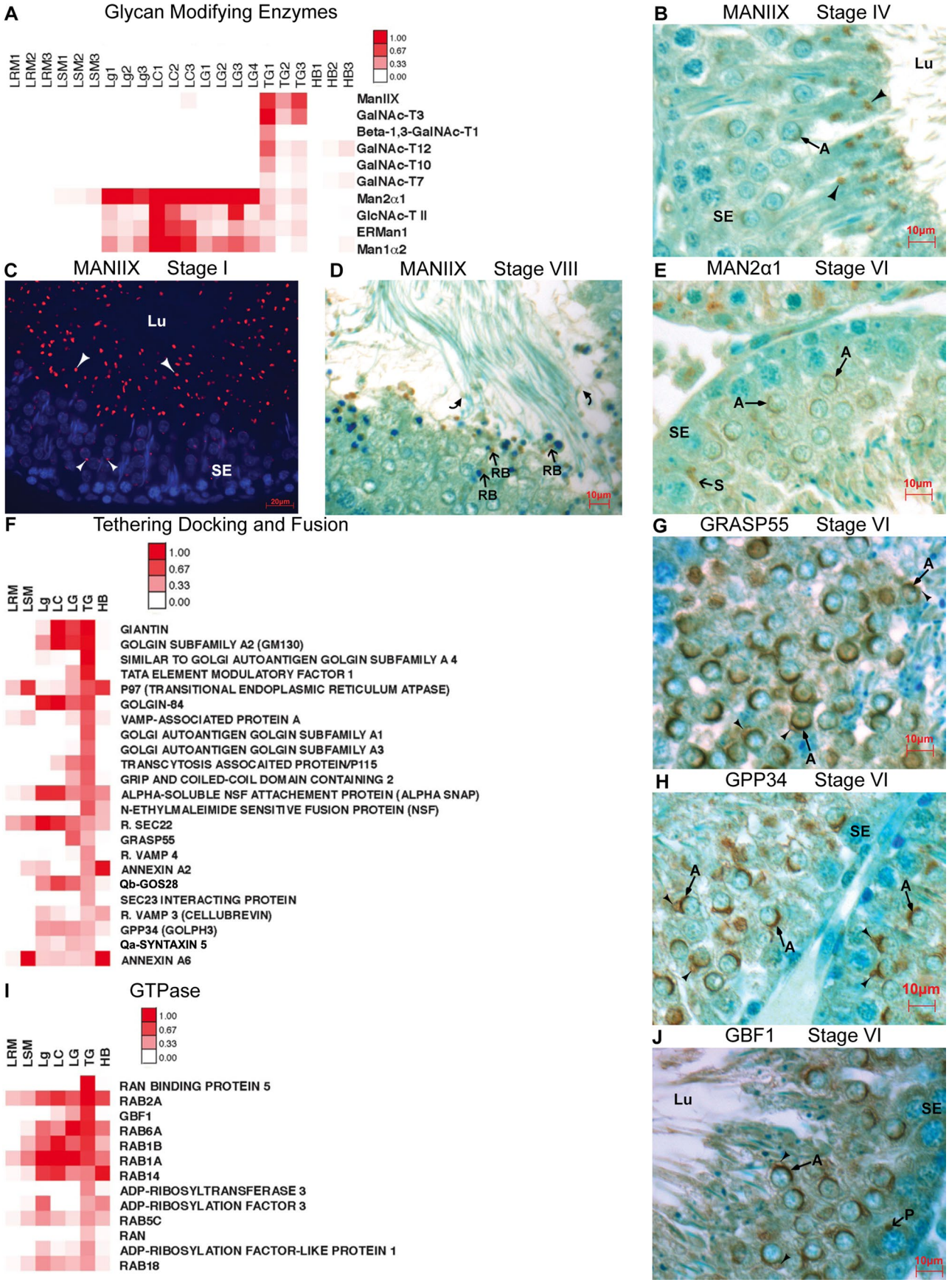

FIGURE 6: Hierarchical clustering and IHC of germ cell–specific Golgi glycan-modifying enzymes, abundant in TG fractions, and tethering, docking, fusion, and GTPase proteins common to somatic cells. (A) Hierarchical clustering of 10 abundant glycan-modifying enzymes enriched in the TG fraction. The plot is by proteins that codistribute across

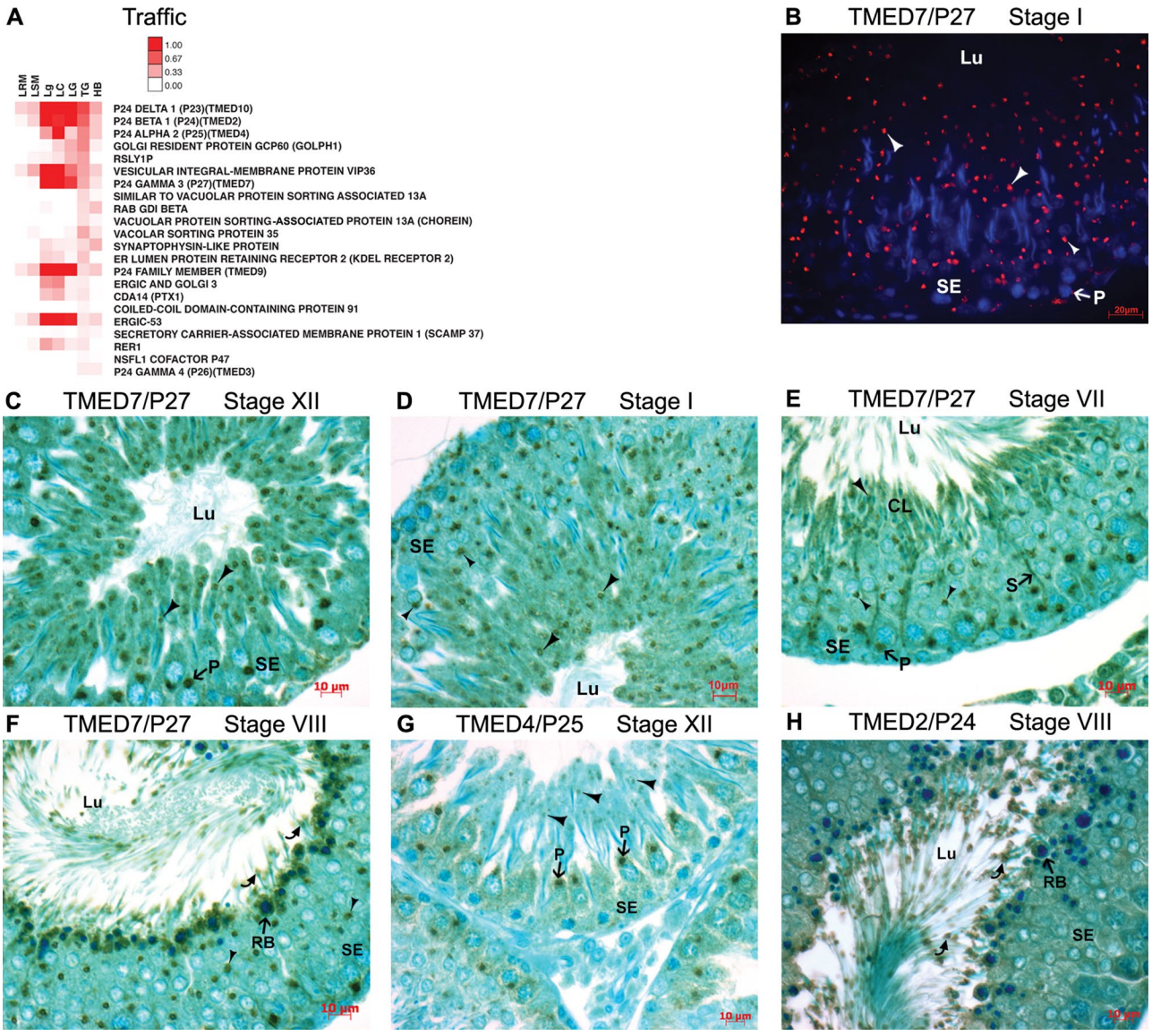

FIGURE 7: TMED/p24 family proteins are abundant trafficking proteins of germ cell Golgi apparatus with differential expression during differentiation. (A) Heat map of 22 proteins of the traffic category sorted by their abundance in the TG fractions. (B) IF and (C–F) IHC for TMED7/p27 throughout germ cell differentiation showing Golgi localizations of early and late germ cells and in the forming Hermes bodies and residual bodies of step 19 spermatids. (G) TMED4/p25 in Golgi apparatus of pachytene spermatocytes and spermatids. (H) TMED2/p24 in the forming Hermes body and residual bodies of step 19 spermatids.

no evidence for its reported Golgi localization as yet. RanBP5 was expressed in the cytoplasm of late step 12–17 spermatids (unpublished data).

Segregation and sorting of Golgi proteins during acrosome formation

In early spermatids, the hemispherical Golgi apparatus is in juxtaposition with the forming acrosome. Immediately thereafter, the Golgi migrates away, as transformations in germ cell differentiation take place (Hermo *et al.*, 2010a). This Golgi migration is readily seen through the Golgi proteins characterized here.

While GL54D, TM9SF3, TMED7/p27, and TMED4/p25 localize to the Golgi apparatus of early spermatids during acrosome formation (Figure 9, A–C), none of these proteins are detected in the acrosome. By contrast, MANIIX (Figure 9D), as well as MAN2α1, GPP34, GBF1, LAMAN, GRASP55, PDILT, sapreticulin, HSP70.2, FAM3C, UBXD8,

different subcellular fractions and not by abundance. (B) IHC of MANIIX shows reaction over acrosomes and Sertoli cells. (C) IF and (D) IHC of MANIIX with reactions over acrosome, germ cell Golgi apparatus, forming Hermes bodies, and residual bodies. (E) IHC of MAN2α1 showing Golgi localization in Sertoli cells and Golgi and acrosomes of germ cells. (F) Heat map of 23 proteins of tethering, docking, and fusion categories sorted by abundance in the TG fraction. (G and H) IHC of GRASP55 and GPP34 (GOLPH3) in Golgi and acrosome of germ cells. (I) Thirteen abundant GTPases sorted by their abundance in TG fractions. Only TG fractions accumulate RanBP5. (J) GBF1 localization to Golgi of pachytene spermatocytes, spermatids, and acrosome.

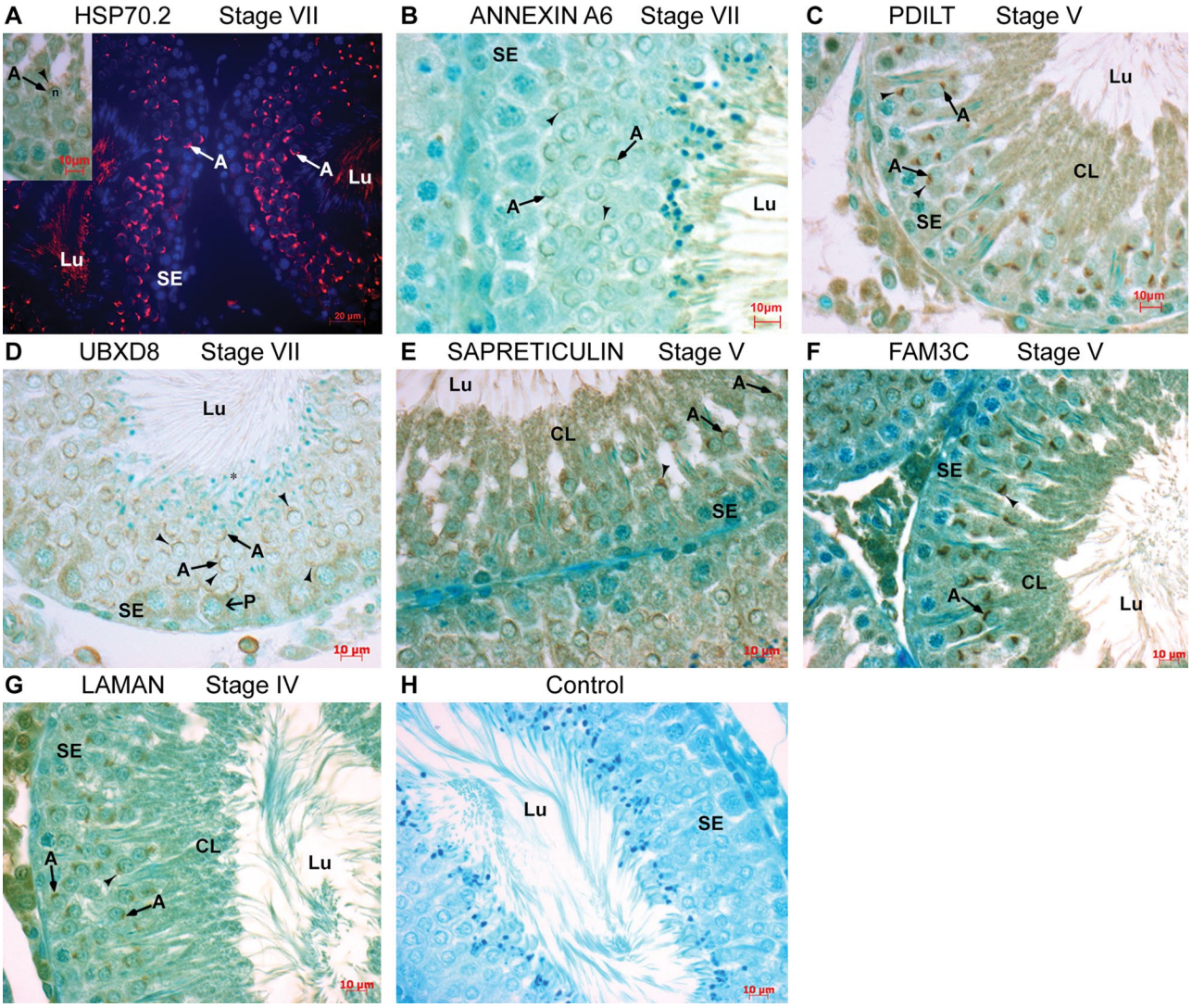

FIGURE 8: Unexpected protein localizations to Golgi and acrosome appear during acrosome formation. (A) IF of HSP70.2 and IHC (inset) show Golgi and acrosome localization. (B) Annexin A6, (C) PDILT, (D) UBXD8, (E) sapreticulin, (F) FAM3C, and (G) LAMAN all show Golgi and acrosome localization in different stages of the cycle. (H) Control without primary antibody.

and annexin A6, are concentrated in both the Golgi apparatus and the developing acrosome of step 1–7 spermatids. At step 8 and onward, when the Golgi apparatus migrates away from the acrosome, GL54D, TM9SF3, TMED7/p27, and TMED4/p25 continue to be localized to the Golgi apparatus and remain undetectable in the acrosome (e.g., Figure 9E for TMED7/p27). However, none of the dual Golgi/acrosome-localized proteins of step 7 spermatids are detectable in the migrating Golgi apparatus at step 8 and in step 9–18 spermatids (e.g., GRASP55, Figure 9F). For those proteins reactive for the acrosome, immunoreactivity is maintained but gradually diminishes by step 15 spermatids. Hence all of these proteins appear to be coincident for acrosome formation and processing of acrosomal enzymes but not for fertilization. The segregation of proteins restricted to the Golgi apparatus or shared between the Golgi and acrosome compartments is depicted in Figure 9G for step 7 spermatids. The differential expression of these proteins during differentiation is illustrated in Figure 5.

Selected Golgi protein expression of spermatocytes, late spermatids, the forming Hermes body, and residual bodies

MG160 is a universal Golgi marker with well-characterized antibodies used by us previously (Dahan *et al.*, 1994; Bell *et al.*, 2001). It is of moderate abundance in the TG fractions (Supplemental Table S1). Unexpectedly, this previously assumed housekeeping Golgi protein (albeit of unknown function) localizes in germ cells only to spermatocytes during meiosis (Figure 10A). This is the first example of the differential expression of MG160 during germ cell differentiation that may be relevant to the process of meiosis, in which the Golgi apparatus dramatically increases in size before division.

Another ubiquitous Golgi protein, sortilin, of far lower abundance by proteomics (Supplemental Table S1), is restricted to germ cells during mid- and late spermiogenesis, that is, after completion of the acrosome and coincident with migration of the Golgi apparatus in late spermatids (Figure 10, B and C). This protein is also prominently expressed in the Golgi apparatus of Sertoli cells at all stages of spermatogenesis (Figure 10, B–D). In step 19 spermatids, immunoreactivity for sortilin segregates completely to the residual body (Figure 10D).

In the epididymis, sortilin is highly expressed in the epididymal epithelial cells but absent from epididymal sperm in the initial segment and caput regions. Oddly, reactivity appears in association with the flagellum of sperm in the corpus and cauda regions (Supplemental Figure 4, A and B). Carboxypeptidase D is an example

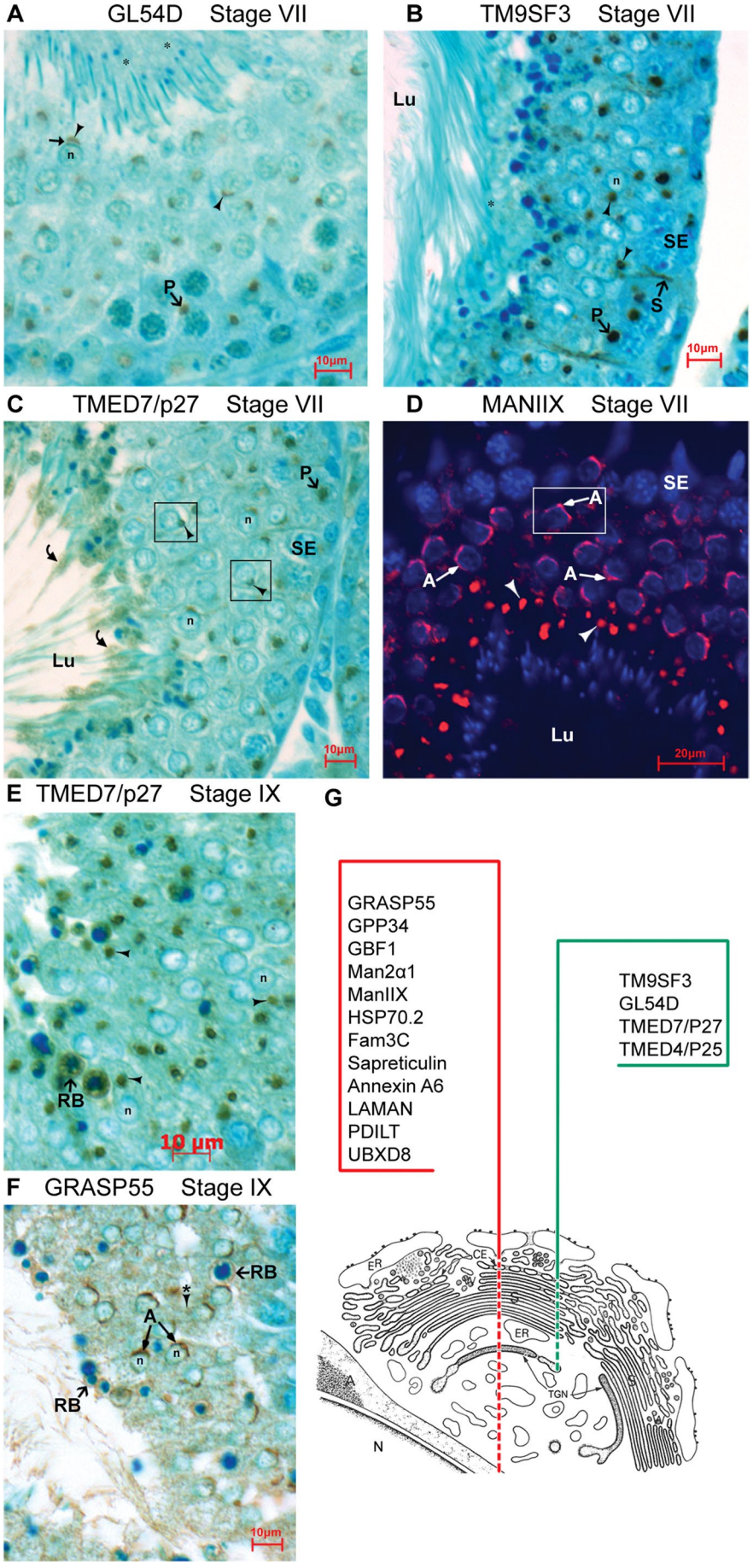

of a Golgi protein with maximal immunoreactivity only in the forming Hermes body in step 19 spermatids (Figure 10E) with maintenance in the Hermes body of epididymal sperm (Supplemental Figure 4C). The expression of these proteins in comparison with all Golgi-localized proteins is summarized in Figure 5.

Not shown is the immunoreactivity of residual bodies immunoreactive for all Golgi-localized proteins in step 19 spermatids. Controls for all experiments are consistently unreactive (e.g., Supplemental Figure 4D).

DISCUSSION

GL54D is the most abundant Golgi-resident protein of spermatocytes and spermatids

Our data represent the first evidence for GL54D as an expressed protein. It is the most abundant protein of the Golgi apparatus of germ cells, validating the method we developed to isolate the germ cell Golgi apparatus. GL54D transcripts are expressed in the testis of mammalian species (Chalmel *et al.*, 2007), but this study represents the first evidence for its expression as a protein and localization in situ exclusive to germ cells of the testis. Although male germ cell specific, the protein localizes to the Golgi apparatus when expressed heterogeneously in liver-derived HepG2 cells.

FIGURE 9: GL54D, TM9SF3, and TMED7/p27 are Golgi restricted, while MANIIX and GRASP55 access the acrosome during germ cell differentiation. (A) GL54D is restricted to the Golgi apparatus (arrowhead) adjacent to the nucleus (n) and apposed to an unreactive acrosome (horizontal arrow). Late spermatids (asterisk) show no immunoreactivity, while the Golgi of pachytene spermatocytes is immunoreactive. (B) TM9SF3 reactive in the Golgi (arrowhead) apposed to an unreactive acrosome. Golgi immunoreactivity in pachytene spermatocytes and Sertoli cells is seen while late spermatids (asterisk) are nonreactive. (C) TMED7/p27 IHC shows reactive Golgi apparatus (boxes in C) without adjacent acrosome immunoreactivity. Golgi localization to pachytene spermatocytes and forming Hermes bodies of step 19 spermatids is seen. (D) IF of MANIIX in acrosome (box) and Golgi apparatus. (E) IHC of step 9 spermatids reactive for TMED7/p27 in the Golgi during its migration. Residual bodies are immunoreactive in step 19 spermatids. (F) GRASP55 showing acrosome but not Golgi immunoreactivity (asterisk over arrowhead) after Golgi migration. (G) Schematic representation of stacks (S) of the Golgi apparatus of the step 7 spermatid overlying the nucleus (N). Proteins localized to both the Golgi and acrosome (red bracket) are indicated. Proteins restricted to Golgi apparatus (green bracket) are shown. The *trans*-Golgi network (TGN), *cis*-Golgi element (CE), and wells (W) of spermatid Golgi apparatus are indicated. Modified from Clermont *et al.* (1995).

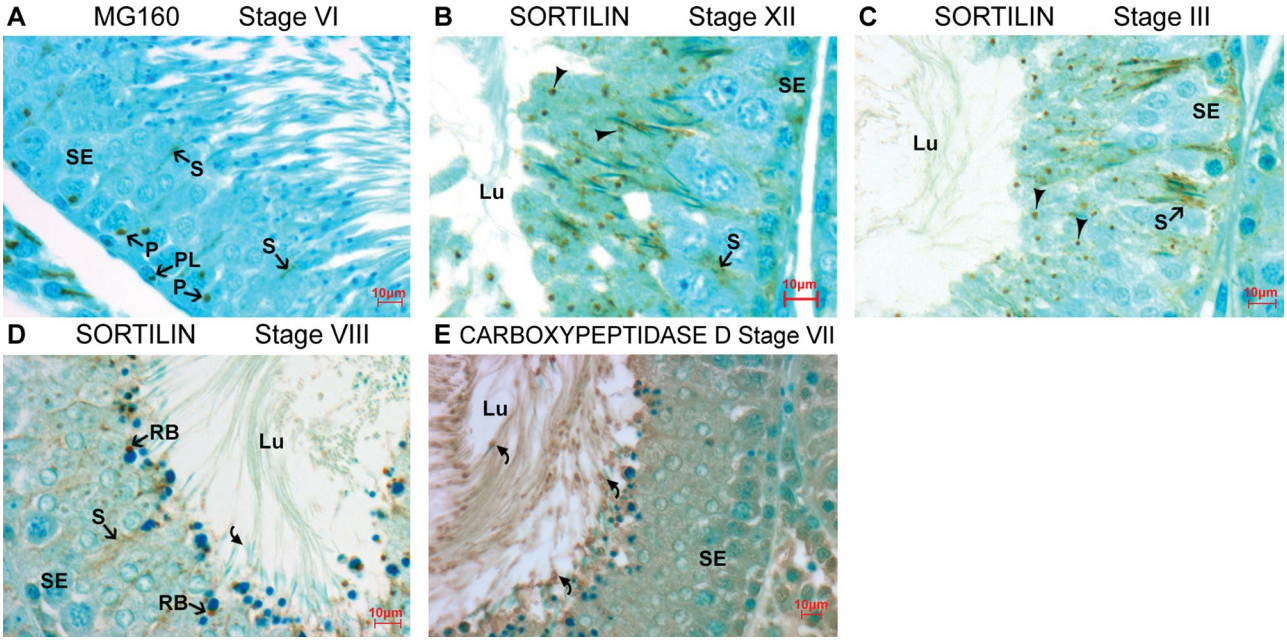

FIGURE 10: Golgi protein expression specific for spermatocytes, late spermatids, and Hermes body formation. Restricted expression of MG160 to spermatocytes, sortilin to postacrosome spermatids, and carboxypeptidase D to step 19 spermatids is noted. (A) MG160 expression is restricted to the Golgi of spermatocytes but present in the Golgi of Sertoli cells (B and C). Restriction of sortilin expression to the late spermatid Golgi with expression also in the Sertoli cell Golgi. (D) Sortilin in residual bodies but absent from forming Hermes bodies. (E) Carboxypeptidase D in forming Hermes bodies.

GL54D is a type II integral membrane protein, which is terminally N-glycosylated and therefore corresponds to the overall features of known Golgi-resident proteins (Nilsson *et al.*, 1994). The function of GL54D is unknown, but it differs from the protein isoform of GL54D named GNT1IP (GlcNAcT-I inhibitory protein; Huang and Stanley, 2010). These authors concluded that this isoform inhibited the activity of GlCNacTransferase1 in germ cells of the mouse testis. However, as indicated by these authors, no transcripts for GNT1P are found in humans or the species under study, here the rat.

A clue to the function of GL54D is revealed by its onset of expression in germ cell differentiation. An exact coincidence of onset of expression of Golgi-localized GL54D with that of the plasma membrane–targeted protein GLUT-3 is observed in pachytene spermatocytes at stage VII of spermatogenesis. The high abundance of GL54D suggests it may select GLUT-3 as well as other germ cell–specific client proteins for their processing and trafficking to the surface of differentiating germ cells in the testis.

TM9 proteins define a new family of abundant Golgi-resident proteins

Uncovered here as a new ubiquitously expressed Golgi marker, TM9SF3 is another abundant protein of poorly understood function. All three TM9 proteins characterized by proteomics may be candidate Golgi markers, as they are highly enriched in liver Golgi but not ER fractions. They are also concentrated in Golgi-derived COPI vesicles, exactly as found for other resident Golgi proteins (Gilchrist *et al.*, 2006). Although prior work suggested a late endosomal to Golgi localization for the expressed tagged protein (Schimmoller *et al.*, 1998) or even plasma membrane localization in yeast (Aguilar *et al.*, 2010), the data here demonstrate an exclusive Golgi localization.

During spermatogenesis, TM9SF3 is undetectable after step 16 spermatids, coincident with the fragmentation of the Golgi ribbon (Susi *et al.*, 1971; Oko *et al.*, 1993). TM9SF3 loss along with that of the highly abundant GL54D during this process is expected to alter profoundly the integrity of the Golgi ribbon as observed. The developmentally regulated stacking, unstacking, and fragmentation of the Golgi ribbon during spermatogenesis should be an optimal model system to uncover the proteins required for Golgi stacking and function (Tulkens and Trouet, 1978; Seemann *et al.*, 2000).

Differential expression and Golgi identity of TMED trafficking proteins

The well-studied TMED proteins (Strating and Martens, 2009; Contreras *et al.*, 2012; Zakariyah *et al.*, 2012) are abundant in the germ cell Golgi apparatus; however, their expression varies for each family member. Expression of TMED7/p27 and TMED2/p24 in the forming and Hermes body of epididymal sperm together define a Golgi identity for the cisternal membranes in epididymal sperm, as demonstrated by others (Moreno *et al.*, 2000a). The expression of TMED proteins is regulated and linked to cargo selection of TMED-enriched vesicular carriers during differentiation (Strating and Martens, 2009; Jerome-Majewska *et al.*, 2010). Although client selection and the specificity for TMED7/p27 in protein transport to the plasma membrane is known for some cells (Liaunardy-Jopeace, 2014), that for the TMED proteins in germ cells is unknown.

Sorting of Golgi-resident proteins during acrosome formation

The immunolocalizations clearly resolved GL54D, TM9SF3, TMED7/p27, and TMED4/p25 proteins to the Golgi apparatus of step 1–7 spermatids but not the tightly apposed developing acrosome. All of these proteins remained associated with the Golgi apparatus as it migrated away from the acrosome during later steps of differentiation with no detection in the acrosome, which remained in association with the nucleus. GL54D, TM9SF3, TMED7/p27, and TMED4/p25 may be considered relevant therefore as defining Golgi identity in germ cells. By contrast, several Golgi-localized proteins were

concentrated in the Golgi apparatus and acrosome (Figure 8B), but these were not detected in the migrating Golgi apparatus after acrosome formation. These proteins remained in the acrosome up to step 15 spermatids, when their immunoreactivity disappeared, presumably due to degradation.

After step 7 spermatids, marking the end of acrosome formation, the innermost Golgi cisternae, *trans*-Golgi networks, disappear from the Golgi ribbon (Susi *et al.*, 1971; Tang *et al.*, 1982). This was also observed in this study. The fact that GL54D, TMED7/p27, TMED4/p25, and TM9SF3 still are identified in the Golgi after step 8 and beyond suggests they are not *trans*-Golgi markers.

The maturation model of Golgi stack anterograde progression has been considered as the model for acrosome formation (Hermo *et al.*, 2010a). However, based on the strict segregation of Golgi markers seen here, alternative models for Golgi traffic and biogenesis cannot be ruled out (Patterson *et al.*, 2008; Dmitrieff and Sens, 2013; Lavieu *et al.*, 2013, 2014).

Acrosome development results from the production and fusion of proacrosomic granules, which assemble on the nucleus commencing at step 1, with added growth to the acrosome in subsequent steps. The TATA element regulatory factor 1 (also known as TMF/ARA160), abundant in the TG fraction, has been suggested to serve as the Golgi protein that binds the proacrosomic granules to the nuclear surface (Lerer-Goldshtein *et al.*, 2010). The data generated in this study also implicate for the first time the Golgi proteins GRASP55, GPP34, and GBF1 and an unexpected role for Fam3C, sapreticulin, annexin A6, UBXD8, PDILT, and HSP70.2 in the protein machinery of acrosome development.

Unconventional Golgi-localized proteins are temporally linked to acrosome biogenesis

Unconventional localization of ER proteins to the Golgi apparatus as seen here for the PDI family member PDILT and sapreticulin during acrosome formation (step 1–7 spermatids) is not unprecedented. The PDI family member erp44 is now accepted to be Golgi localized in most cell types, but its localization changes to the ER dependent on its cargo (Gannon *et al.*, 2011; Smirle *et al.*, 2013). A known PDILT client in germ cells is the acrosome-located membrane protein ADAM3 (Linder *et al.*, 1995; Tokuhiro *et al.*, 2012). However, after acrosome formation, PDILT in late elongating spermatids relocalizes to the ER (van Lith *et al.*, 2007; Tokuhiro *et al.*, 2012). Hence it is the PDILT client proteins that likely dictate its localization in the secretory pathway.

The saposin B domain–containing protein sapreticulin localizes to the acrosome and Golgi of step1–7 spermatids in testis (Figures 7E and 8G). Spermatids are devoid of prosaposin (Hoskins *et al.*, 1978), leaving sapreticulin as the only saposin domain–containing protein in germ cells. The Golgi-localized sulfoglycolipids (Fujiwara *et al.*, 2013) are predicted potential clients of sapreticulin.

Golgi-localized HSP70.2 may function in clathrin-coated vesicle trafficking known to be prominent during acrosome formation (Griffiths *et al.*, 1981). Such clathrin uncoating is well described for the somatic counterpart to HSP70.2, that is, Hsc70 (Bocking *et al.*, 2011). Localization to the cytoplasm of germ cells has been reported when a different antibody has been used, with different functions deduced (Rosario *et al.*, 1992; Eddy, 1999). Whether this reflects the different epitopes recognized by these antibodies has not been resolved. Nevertheless, the recruitment of chaperones (HSP), protein-folding enzymes (PDILT), and ERAD (endoplasmic reticulum-associated protein degradation) quality-control proteins (UBXD8) to the Golgi apparatus must assure the fidelity of sorting and transport of proteins during acrosome biogenesis.

MANIIX and sortilin expression and the remodeling of late spermatid morphology

Once acrosome formation ceases in step 7 spermatids, the Golgi apparatus migrates away from the acrosome toward the cytoplasmic lobe of step 8 and later spermatids. Two proteins, MANIIX and sortilin, are expressed in the Golgi apparatus at late steps of spermiogenesis. The surge of MANIIX expression in the Golgi apparatus from steps 15 to 19 is likely relevant to glycosyl modifications for glycan-mediated germ/Sertoli cell associations and other events crucial for spermatogenesis and fertility (Fukuda and Akama, 2002, 2003a,b; Batista *et al.*, 2012).

After acrosome formation, Man-6-P receptor expression diminishes (O'Brien *et al.*, 1994; Chayko and Orgebin-Crist, 2000). As shown here, this coincides with the onset of expression of the Golgi sorting receptor sortilin. A wave of sortilin expression in the Golgi apparatus appears from steps 8 to 19. Coincidently, at step 8, a marked diminishment in surface-located GLUT-3 is observed. Because sortilin is known to regulate GLUT-4 sorting (Hatakeyama and Kanzaki, 2011; Huang *et al.*, 2013), a similar role for sortilin here in the GLUT-3 sorting from step 8 and onward is predicted. Hence sortilin expression in the late Golgi apparatus coincides with postacrosome Golgi migration and a remodeling of the plasma membrane (Clermont and Tang, 1985; Clermont *et al.*, 1993). Elucidation of the germ cell–specific sortilin clients may provide further insight for its differential expression.

The step 19 spermatid

Transcription ceases immediately after acrosome formation, with protein expression thereafter under translational regulation (Hecht, 1990). The translation-controlled pathway for organelle modification and morphogenesis of germ cells (Chappell *et al.*, 2013) must be prominent at step 19, since a burst of Golgi protein expression is seen at this terminal step of germ cell development (summarized in Figure 5). This concurs with the exclusive expression of non Golgi proteins, as evidenced in Au *et al.* (2015).

The segregation of the residual body from the forming Hermes body takes place in step 19. While it has been suggested that the Golgi ribbon undergoes fragmentation after step 15 (Susi *et al.*, 1971; Tang *et al.*, 1982), MANIIX and sortilin are expressed in a large spherical entity in later spermatids and as distinct reactive clumps ending up in the residual body. Indeed, all the Golgi-localized proteins in step 19 are also immunoreactive in the residual body, albeit of differing diffuse intensities. The residual body appears to sort and segregate subcompartments of the Golgi ribbon. Further studies are needed to test the segregation of proteins related to unstacked cisternae in the forming Hermes body versus those of the intermediate compartment, *cis*-Golgi network, and tubular interconnecting regions that may reside in the residual body.

An important function occurring in step 19 spermatids is their individualization into spermatozoa by disruption of the syncytium formed by intercellular bridges (Dym and Fawcett, 1970; Greenbaum *et al.*, 2009). It is attractive to propose the internal membranes of the forming Hermes body as the source of new plasma membrane to seal off each individual spermatid, resulting in spermatozoa.

Proteins of unknown function

In addition to GL54D and TM9 family members, there are 240 characterized proteins of unknown function in the TG fractions. A complete understanding of the Golgi apparatus may await the protein-by-protein elucidation of mechanisms of the known and the 240 unknown proteins deduced here. When complemented by their

differential expression during germ cell differentiation, as shown for the 20 proteins localized here, then a complete elucidation of the Golgi apparatus may be at hand.

Conclusion

Through the isolation of a germ cell Golgi fraction from whole testis homogenates, GL54D is uncovered as the most abundant Golgi-resident protein and germ cell specific. The TM9 family is uncovered as new Golgi markers for all cells. The sorting and segregation of Golgi markers during acrosome formation is uncovered, and the differential expression of 20 different Golgi-localized proteins is observed during germ cell differentiation, coincident with major changes in germ cell Golgi structure, location, and function.

MATERIALS AND METHODS

Animals

All animals (Sprague Dawley rats) used in this study were maintained on a 12-h dark/light cycle in the animal facility and fed ad libitum. The procedures for animal use were done in accordance with the guidelines of the McGill Animal Care Committee.

Isolation and characterization of germ cell Golgi fraction from adult rat whole testis

All adult Sprague Dawley rats (350–450 g) were purchased from Charles River Laboratories Canada (St. Constant, QC). For each isolation procedure, 10 rats were used. After anesthesia, the testes were removed from the scrotum following intracardiac saline perfusion.

The strategy designed to isolate the stacked Golgi apparatus from rat liver parenchyma (Dominguez *et al.*, 1998) was used as a starting point and then modified to isolate stacked cisternae of the Golgi apparatus from rat testes. The principle was to utilize a gentle homogenization protocol to assure maximal stacking of Golgi cisternae and a minimum of fragmentation of the isolated Golgi apparatus. Because the spermatocyte and spermatid Golgi apparatus are both compact (largely spherical) and have the most cisternae (~9–12) of any cell type in testis, they were expected to sediment rapidly. Therefore, after gentle homogenization followed by low-speed differential centrifugation, pellets were recovered and resuspended gently and the Golgi fractions were isolated from discontinuous gradients.

The final method was as follows: after saline perfusion, rat testes were removed from the scrotum through the abdominal cavity and kept at 4°C. The capsule surrounding the testes was removed, and the contents were homogenized in ice-cold buffer (5 mM Tris-HCl, pH 7.4, 25 mM KCl, 1 mM phenylmethylsulfonyl fluoride [PMSF]), 200 K units of aprotinin per ml of buffer) by 10 up- and downstrokes of a loose Dounce homogenizer. The 10 rats used per experiment ($n = 3$) corresponded to ~13 g of testes, with the final amount of testis-to-buffer corresponding to 20% weight by volume. The homogenate was filtered through two layers of cheesecloth to remove connective tissue. This filtered homogenate was centrifuged at 400 × *g* maximum (850 rpm; Avanti R-20 rotor [Beckman Coulter, Mississauga, Canada]) for 5 min. The supernatant (S1) was saved, and the pellet (P1) rehomogenized in half the original volume of buffer, with 5 up- and downstrokes of a loose Dounce homogenizer, and then centrifuged at 400 × *g* maximum for 5 min. This pellet (P2) was set aside. The supernatant (S2) was combined with S1, and the combined supernatants were centrifuged at 1500 × *g* maximum (3500 rpm; Avanti R-20 rotor) for 10 min. The pellet (P3) was combined with the reserved P2 and resuspended at 20% weight by volume in buffer (1.22 M sucrose 5 mM Tris-HCl, pH 7.4, 25 mM KCl, 1 mM PMSF, 200 K units of aprotinin per ml of buffer) with 3–5 strokes of a loose Dounce homogenizer.

The resuspended pellets were placed in SW-28 tubes (18 ml per tube); this was followed by layering of 10 ml of buffered 1.1 M sucrose and then a layer of 8–10 ml of buffered 0.5 M sucrose. Tubes were centrifuged for 30 min at 3000 rpm (1191 × *g* average), followed by 25000 rpm (74,000 × *g* average) for 1 h with the brake on. The band at the interface of 1.1 M and 0.5 M sucrose was collected and adjusted to 0.4 M sucrose with additional buffer. This was centrifuged at 1500 × *g* maximum for 10 min. The supernatant (S4) was discarded, and the pellet (P4) was resuspended in 6 ml of buffered 1.25 M sucrose and underlaid beneath a step gradient of equal volumes of buffered sucrose (1.1 M/1.0 M/0.6 M) and centrifuged at 40,000 rpm (202,000 × *g* average) for 35 min (SW-40 rotor) with the brake on. The band at the interface of 1.1 M/1.0 M sucrose was collected without pelleting and characterized. The isolated Golgi fraction was enriched 33.5-fold ± 6.3 (mean ± SD, $n = 4$) for the marker enzyme UDP-galactose ovomucoid-galactosyltransferase as compared with the starting whole testis homogenate and accounted for 0.04% ± 0.02% (mean ± SD, $n = 3$) of the starting homogenate protein.

The design of the final discontinuous gradients (above) was based on prior experiments with continuous gradients as follows: after the generation of the S1 and S2 fractions (above), S1 and S2 were combined and centrifuged at 45,000 rpm (144,000 × *g* average) in a 60Ti rotor for 40 min. The resulting pellet was resuspended in homogenization buffer (1 ml/g wet weight of testis). One-half milliliter was placed on top of a continuous gradient of 0.7 M to 1.8 M sucrose in homogenization buffer and centrifuged at 25,000 rpm (79,000 × *g* average) in an SW-40 rotor for 17 h. One-milliliter fractions were collected for protein determination and Western blots for calnexin, MG160, TMED11 (gp25L), GL54D (unpublished data) as well as enzyme assays for galactosyltransferase. This enabled the design of the discontinuous gradient for the selection of a Golgi-enriched fraction (median density of 1.12 g/ml).

Routine EM processing of in situ testis and isolated subcellular TG fractions

For routine EM analysis, four adult male Sprague Dawley rats were anesthetized with sodium pentobarbital, and their testes were fixed by perfusion through the abdominal aorta with 2.5% glutaraldehyde in 0.2 M sodium cacodylate buffer containing 0.1% calcium chloride (pH 7.4; Hermo *et al.*, 1988). After fixation (10 min), the tissue was removed, trimmed, and left in fixative for 2 h. It was then postfixed in potassium ferrocyanide–reduced osmium tetroxide for 1 h, after which it was dehydrated in alcohol and acetone and embedded in Epon. Sections were cut with a diamond knife, stained with uranyl actetate and lead citrate, and examined with a Philips 400 EM, Tecnai 12 120kV TEM and Tecnai G2 F20 Cryo-STEM (FEI, Hillsboro, OR).

For isolated TG fractions, a portion of each sample from $n = 3$ isolated fractions was processed for EM analysis. Two milliliters of isolated subcellular fractions (100–150 µg protein) in ice-cold buffer was mixed with 2 ml of fixative (5% glutaraldehyde in 0.2 M sodium cacodylate buffer containing 0.1% calcium chloride, pH 7.4) on ice in a chemical fume hood. The TG fractions were collected onto filter membranes (nitrocellulose filter 0.45 mm HA; Millipore), washed with 0.1 M cacodylate buffer (pH 7.4, containing 5% sucrose) three to four times, incubated with tannic acid (1% tannic acid in 0.1 M cacodylate buffer, pH 7.4) for 1 h, washed with cacodylate buffer containing 1% sodium sulfate, placed in 100 mM maleate buffer (pH 5.7), incubated with uranyl acetate (6% uranyl acetate in 0.1 M sodium

maleate, pH 5.7) for 2 h on ice in the fume hood, washed with maleate buffer, dehydrated through a series of graded alcohols (70, 80, 90, 95, and 100% ethanol) 10 min for each step, and then dissolved in 100% acetone for 1–2 h. The samples were embedded in Epon resin, and the blocks were then cut and sectioned (90–100 nm), stained with uranyl acetate and lead citrate, and examined with a Tecnai 12 120 kV TEM equipped with a Gatan 792 Bioscan CCD Camera (Gatan, Pleasanton, CA).

EM of the isolated TG fraction revealed, in random views (Baudhuin *et al.*, 1967), a homogenous preparation of stacked Golgi cisternae with up to nine cisternae forming a stack exactly as seen for the spermatocyte/spermatid Golgi apparatus in situ but very different from the Golgi apparatus of Sertoli cells or Leydig cells of the testis, which are not spherical in shape and are composed of approximately five flattened cisternae in a stack. By morphometry (Bell *et al.*, 2001), of $n = 4$ isolates, 51.6% ± 13.3% of the membranous structures were stacked Golgi apparatuses (i.e., 1287 Golgi apparatuses in 11 micrographs at an EM magnification of 1900×). Anything elongated in the shape of a cisternae, stacked or not, was considered as "Golgi." Depending on the preparation, the proportion of stacks was variable. Some had many stacks of three to four cisternae, others had only a single cisterna. Any vesicle associated with or contacting a cisterna was considered as "Golgi," as were vesicles that appeared to touch a cisterna or to touch other vesicles that touched a cisterna. Vesicle clusters not associated with cisternae were not considered Golgi.

Electron microscope tomography

Samples were prepared as described above. However, thicker sections (~250 nm) were cut for electron tomography and transferred onto carbon-coated copper grids. Images were collected on a Titan Krios microscope operated at 300 kV using a Gatan Ultrascan 4k × 4k CCD camera. For electron tomography, data collection was done at an electron dose of ~1500 electrons/Å^2 per tomogram. Focusing was done on an adjacent area to minimize electron dose exposure. In total, more than 30 tomograms were collected at different magnifications ranging between 20k and 50k. Tilt series were taken using the FEI software in the angular range between −64° and +64° with 2o increments. For the estimated sample thickness, this would be sufficient for a resolution of 2 nm, following the Crowther formula. Reconstruction of three-dimensional volumes was done using the IMOD software suite (Kremer *et al.*, 1996). The final tomograms were binned three times in to increase the signal-to-noise ratio. Three-dimensional rendering was done using Chimera (Pettersen *et al.*, 2004).

Transfection and selection of stable clones

The GL54D-GFP construct used in this study was from *Rattus norvegicus* cDNA clone MGC: 114453 IMAGE: 7454086. The PCR product of the image clone was inserted between *Xho*I and *Sac*II sites in the EGFP-N1 vector, producing a linker of 10 amino acids PRARDPPVAT between N-terminal GL54D and C-terminal EGFP. The primers used in the PCR were as follows: forward 5′-GATCTCGAGACCATGAAGACCAAGAACGTTAAC-3′ and reverse 5′-GATCCGCGGGTAGTAATGATCCTTGAGGTGCTGTTC-3′. HepG2 cells were transfected using Fugene HD (Roche Diagnostics, Laval, Canada), and stable clones were selected with G418 6 mg/ml for 2 wk and continued culture with G418 for another 3 mo before imaging analysis.

Cell culture, indirect IF, and confocal microscopy

HepG2 cells were grown on coverslips at 30,000 cells/coverslip for 24 h. Cells were fixed with 3% paraformaldehyde in phosphate-buffered saline (PBS) for 15 min and were washed with PBS three times for 5 min for each wash at room temperature. Cells were blocked and permeabilized with PBS containing 0.2% fish skin gelatin (PBS-G; Sigma-Aldrich Canada, Mississauga, Canada) and 0.1% saponin (Sigma-Aldrich) for 30 min at room temperature. Primary antibodies were diluted in PBS-G, and the cells were incubated for 1 h at room temperature. Cells were then washed three times for 5 min each wash in PBS-G and incubated with secondary fluorophores diluted 1:1000 in PBS-G for 30 min at room temperature. Cells were again washed, and coverslips were mounted onto glass slides using ProLong Gold Antifade mounting media (Invitrogen). All images were acquired using an LSM 700 series microscopy system (Carl Zeiss) fitted with a Plan-Apochromat 63×/1.40 oil-immersion objective in sequential-scanning mode with the pinhole set to obtain an optical section of ~0.8 µm in both channels (1 Airy unit). For GFP, a 488-nm argon ion laser was used, and emitted fluorescence was filtered through a 505- to 530-nm band-pass filter. Alexa Fluor 568 and 647 were excited with a 561-nm DPSS laser and a 633-nm laser line, respectively, and the emitted fluorescence was filtered through a 585- to 690-nm band-pass filter for Alexa 568 and a 580-nm long-pass filter for Alexa 647. For live-cell imaging, cells were grown as above but in MatTek dishes (MatTek, Ashland, MA) and imaged as above under normal cell culture conditions (i.e., CO_2, humidity, and temperature).

Antibody production

Rabbit polyclonal antibodies produced "in house" for this study were generated using standard procedures to the peptide sequences indicated in the legend to Supplemental Table S2. Specificity of the antibodies was tested by Western blotting on isolated testis and rat liver Golgi fractions (unpublished data). All other antibodies were obtained from the labs indicated in Supplemental Table S2 and have been highly characterized by these investigators for specificity and immunoreactivity. For all in-house antibodies, the indicated peptide sequences were used to generate polyclonal antibodies as indicated in Ou *et al.* (1993).

Triton X-114 phase partitioning, glycosidase digestions, and Western blotting

Triton X-114 phase partitioning of TG fractions was based on that done for subcellular fractions in Gilchrist *et al.* (2006). Digestions of TG fractions with PNGase F, EndoH, and Neur + O-Glyco were performed according to the manufacturer's instructions (New England Biolabs). Proteins were resolved on 10% Laemmli SDS–polyacrylamide gels, and Western blot analysis was performed using the anti-GL54D antibody followed by horseradish peroxidase–conjugated protein A (Bio-Rad Laboratories Canada Ltd., Mississauga, Canada) and enhanced chemiluminescence (ECL; Perkin Elmer Biosignal, Montreal, Canada). Bands were then visualized by exposure of the blot to Kodak Biomax MR-2 film (Sigma-Aldrich).

Tandem mass spectrometry

The methodologies described in Gilchrist *et al.* (2006) and Bell *et al.* (2009) were followed. The raw data were processed in pipeline format (Bencsath-Makkai *et al.*, 2003) to generate a peaklist of all tandem mass spectrometry (MS) by employing Distiller followed by Mascot Cluster. The Mascot search results were then parsed into the in-house relational database termed CellMapBase (Bencsath-Makkai *et al.*, 2003), scored for protein identifications, and grouped to present a minimum set of protein identifications (Kearney *et al.*, 2005) to account for all tandem MS assigned at 95% confidence. The concatenated peaklist was searched against a copy of the

National Center for Biotechnology Information nonredundant database (ftp://ftp.ncbi.nih.gov/blast/db/FASTA/nr.gz, release: NCBI nrdb 2008). For generation of the minimum list of proteins (Kearney *et al.*, 2005), protein identifications were grouped based on redundant peptide assignments, taking into account redundancies that arise due to homologous sequences, truncated or partial sequences, alternatively spliced proteins, strain-specific allelic variation, or redundant assignments of tandem MS. In this process, peptides were assigned as unique to identification or shared between two or more identifications. For quantification, redundant peptide counting (spectral counts) was performed essentially as described previously (Blondeau *et al.*, 2004; Liu *et al.*, 2004; Gilchrist *et al.*, 2006; Bell *et al.*, 2009). In the present case, peptides were grouped to their cognate proteins based on the gel-resolved sample, and shared peptides were apportioned to the cognate proteins based on the proportion of unique peptides. For comparison between samples, normalized (based on Total Peptides assigned in that biological repeat)% Total Peptides for $n = 3$ or 4 (Supplemental Table S1) were used.

Data analysis

As indicated in the preceding section, all protein identifications made by peptides assigned by Mascot at the 95% confidence level (false-positive rate ~1.5% estimated by searching a randomized copy of the database for the legacy data; Gilchrist *et al.*, 2006) were tabulated into a relational database (CellMapBase) for further manipulations as described in Au *et al.* (2015). Proteins are indicated by their relative abundance in the TG fraction, Supplemental Table S1.

Hierarchical clustering

Hierarchical clustering was done using the Cluster 3.0 program (bonsai.hgc.jp/~mdehoon/software/cluster; de Hoon *et al.*, 2004), and clusters were viewed by the JAVA TREEVIEW program (http://jtreeview.sourceforge.net; Eisen *et al.*, 1998). Microsoft Excel was used for all data analysis.

Light microscope immunocytochemistry

The testes and epididymides of adult rats used for LM-IHC and in some cases LM-IF were fixed by perfusion through the abdominal aorta for 10 min, after which the tissues were left overnight in fresh fixative (Hermo *et al.*, 1988), or by simple immersion in Bouin's for 24 h (n = 4 for each) at room temperature. Other rats were fixed by perfusion or immersion ($n = 2$ for each) with zinc fixative (cat no. 550523; BD Biosciences, Mississauga, Canada; Hermo *et al.*, 2008). On removal from the animal, the testis was cut in half. After fixation, the tissues were subsequently placed in 70% alcohol for several days before being dehydrated and embedded in paraffin.

Paraffin sections were cut at a 5-µm thickness and mounted on "Posi-Plus" slides (Fisher Scientific Company, Ottawa, Canada). Sections of testis tissue were deparaffinized with Histoclear (Fisher brand 22–143975; Fisher Scientific, Ottawa, Canada) and rehydrated in a series of 100, 95, 80, 70, and 50% ethanol solutions; 0.3 M glycine; and PBS.

Following rehydration, immunostaining was performed with the Envision+ System-HRP (DAB, diaminobenzidine) anti-rabbit Kit (cat no. K4010; Dako Canada, Mississauga, Canada) and a wash buffer solution containing 0.05 M Tris, 0.3 M NaCl, and 0.1% Tween 20 (pH 7.4). Dilutions for each primary antibody (using 5% bovine serum albumin in PBS) were optimized and fell within a range of 1:100–1:500 and were incubated on the slides at room temperature for 1.5 h. Slides were washed 10× for 1 min each wash and incubated with the secondary antibody, (Envision+ kit) for 60 min at room temperature. The slides were again washed for 10× for 1 min and incubated with the DAB solution from the Envision+ kit (time of incubation was optimized for each protein and fell into the range of 5–30 s). The sections were counterstained for 10 s in methylene blue, washed, and quickly dehydrated through graded ethanol solutions to Histoclear. Coverslips were mounted onto the slides with Permount.

Negative controls for all experiments consisted of substituting PBS for primary antibody. Negative control experiments were performed using the above protocol, but without primary antibody. Nonimmune sera were also substituted for primary antibody as control, with no immunoreactivity detected. When available (e.g., anti-GL54D), preimmune sera were also tested and shown to have no detectable immunoreactivity.

Antibody localizations

While the LM-IHC/IF data are qualitative, each antibody was subjected to extensive morphological analysis. Both Bouin- (LM-IHC; $n = 4$ adult rats) and zinc- (LM-IF; $n = 2$ adult rats) fixed testes from adult rats were analyzed for each antibody. At least four replicas for each antibody were done for Bouin-fixed material and, in some cases, as many as 20 replicas were done. For LM-IF, at least two replicas were done, but only a few selected antibodies were examined. For LM-IHC, the results are based on ~450 different slides, of which ~120 were controls. For each antibody, the data took into account all 14 stages of the cycle of the seminiferous epithelium in the testis, as well as an analysis of epididymal sperm from the four major regions of the epididymal duct. Thus, while qualitative, the data were reproducible for each antibody as deduced by different fixatives, animals, and controls and over the 20 personnel involved with the LM immunolocalizations.

IF

Sections were deparaffinized in hexane (Fisher Scientific), rehydrated in a graded ethanol series, and washed in distilled water followed by 50 mM Tris-buffered saline (TBS; pH 7.4). Sections were incubated for 3 h at room temperature with primary antibody diluted as above in TBS. Sections were washed with TBST (TBS + 0.1% Tween 20), blocked for 20 min in a 2% casein solution, and incubated for 30 min at room temperature with Alexa Fluor 594–labeled goat anti-rabbit immunoglobulin G antibody (Invitrogen Canada, Burlington, Canada) diluted 1:500 in TBST. Samples were washed with TBST, rinsed in TBS, and counterstained for 1–3 min at room temperature with 300 nM 4′,6-diamidino-2-phenylindole dihydrochloride (Invitrogen Canada) in TBS. Samples were rinsed in TBS, and coverslips were mounted using ProLong Gold Antifade reagent (Invitrogen Canada). Sections were examined and photographed on a Zeiss Axioskop 2 motorized light microscope equipped with variable intensity FluorArc epifluorescence mercury lighting and an AxioCam HR color digital camera (Carl Zeiss Canada, Montreal, QC, Canada). Controls were done as indicated above.

For LM-IF of tissue sections, the results are based on 35 slides, with an additional 10 as controls. Seven antibodies were examined by LM-IF.

ACKNOWLEDGMENTS

We thank FEMR (www.medicine.mcgill.ca/femr) for EM services (Jeannie Mui) and Kaustuv Basu and Mihnea Bostina for EM tomography. Daniel Friedman, Kristyn Malcolm, Zariyat Mannan, Rebecca Richard, Carl Dahlen, Nadiya Goswami, Abigail Belasen, Maria-Teresa Eyzaguirre, Aurore Fonderflick, Sohee Kang, Dru Perkins,

Andrea Prince, Jason Lee, Raja Talla, Rachel Adilman, and Adam Parent contributed by assisting with IHC. We are especially grateful to the investigators indicated in Supplemental Table S2 (Au *et al.*, 2015), who generously provided antibodies and advice and guided us to commercial antibodies when available. We thank Hana Hakami (King Saud University) for her comments and help in the preparation of the manuscript. This work was supported by CIHR grant MOP 5605. This paper is dedicated to Yves Clermont and C. P. Leblond, who elaborated the stem cell renewal theory for male germ cell differentiation (www.mcgill.ca/anatomy/stem-cell-renewal-theory).

REFERENCES

Aguilar PS, Frohlich F, Rehman M, Shales M, Ulitsky I, Olivera-Couto A, Braberg H, Shamir R, Walter P, Mann M, *et al.* (2010). A plasma-membrane E-MAP reveals links of the eisosome with sphingolipid metabolism and endosomal trafficking. Nat Struct Mol Biol 17, 901–908.

Au CE, Hermo L, Byrne E, Smirle J, Fazel A, Kearney RE, Smith CE, Vali H, Fernandez-Rodriguez J, Simon PHG, *et al.* (2015). Compartmentalization of membrane trafficking, glucose transport, glycolysis, actin, tubulin and the proteasome in the cytoplasmic droplet/Hermes body of epididymal sperm. Open Biol 5, 150080.

Batista F, Lu L, Williams SA, Stanley P (2012). Complex N-glycans are essential, but core 1 and 2 mucin O-glycans, O-fucose glycans, and NOTCH1 are dispensable, for mammalian spermatogenesis. Biol Reprod 86, 179.

Baudhuin P, Evrard P, Berthet J (1967). Electron microscopic examination of subcellular fractions. I. The preparation of representative samples from suspensions of particles. J Cell Biol 32, 181–191.

Bell AW, Deutsch EW, Au CE, Kearney RE, Beavis R, Sechi S, Nilsson T, Bergeron JJ (2009). A HUPO test sample study reveals common problems in mass spectrometry-based proteomics. Nat Methods 6, 423–430.

Bell AW, Ward MA, Blackstock WP, Freeman HN, Choudhary JS, Lewis AP, Chotai D, Fazel A, Gushue JN, Paiement J, *et al.* (2001). Proteomics characterization of abundant Golgi membrane proteins. J Biol Chem 276, 5152–5165.

Bencsath-Makkai Z, Bell A, Bergeron J, Boismenu D, Funnell R, Harrison M, Paiement J, Roy L, Kearney R (2003). Information system for high-throughput proteomics: CellMapBase. Mol Cell Proteomics 2, 833.

Bencsath-Makkai Z, Bell A, Bergeron J, Boismenu D, Harrison M, Funnell WRJ, Mounier C, Paiement J, Roy L, Kearney RE (2003). CellMapBase—an information system supporting high throughput proteomics for the Cell Map Project. IEEE EMBS 4, 3567–3570.

Blondeau F, Ritter B, Allaire PD, Wasiak S, Girard M, Hussain NK, Angers A, Legendre-Guillemin V, Roy L, Boismenu D, *et al.* (2004). Tandem MS analysis of brain clathrin-coated vesicles reveals their critical involvement in synaptic vesicle recycling. Proc Natl Acad Sci USA 101, 3833–3838.

Bocking T, Aguet F, Harrison SC, Kirchhausen T (2011). Single-molecule analysis of a molecular disassemblase reveals the mechanism of Hsc70-driven clathrin uncoating. Nat Struct Mol Biol 18, 295–301.

Bonifacino JS, Hurley JH (2008). Retromer. Curr Opin Cell Biol 20, 427–436.

Chalmel F, Rolland AD, Niederhauser-Wiederkehr C, Chung SS, Demougin P, Gattiker A, Moore J, Patard JJ, Wolgemuth DJ, Jegou B, Primig M (2007). The conserved transcriptome in human and rodent male gametogenesis. Proc Natl Acad Sci USA 104, 8346–8351.

Chappell VA, Busada JT, Keiper BD, Geyer CB (2013). Translational activation of developmental messenger RNAs during neonatal mouse testis development. Biol Reprod 89, 61.

Chayko CA, Orgebin-Crist MC (2000). Targeted disruption of the cation-dependent or cation-independent mannose 6-phosphate receptor does not decrease the content of acid glycosidases in the acrosome. J Androl 21, 944–953.

Christensen AK (1975). Leydig cells. In: Handbook of Physiology, ed. RO Greep and EB Astwood, Washington, DC: American Physiological Society, sect. 7.

Clermont Y (1972). Kinetics of spermatogenesis in mammals: seminiferous epithelium cycle and spermatogonial renewal. Physiol Rev 52, 198–236.

Clermont Y, Hermo L, Oko R (1993). Cell Biology of Mammalian Spermiogenesis. In: Cell and Molecular Biology of the Testis, ed. C Desjardins and LL Ewing, New York: Oxford University Press, chap. 14.

Clermont Y, Rambourg A, Hermo L (1995). Trans-Golgi network (TGN) of different cell types: three-dimensional structural characteristics and variability. Anat Rec 242, 289–301.

Clermont Y, Tang XM (1985). Glycoprotein synthesis in the Golgi apparatus of spermatids during spermiogenesis of the rat. Anat Rec 213, 33–43.

Contreras FX, Ernst AM, Haberkant P, Bjorkholm P, Lindahl E, Gonen B, Tischer C, Elofsson A, von Heijne G, Thiele C, *et al.* (2012). Molecular recognition of a single sphingolipid species by a protein's transmembrane domain. Nature 481, 525–529.

Dahan S, Ahluwalia JP, Wong L, Posner BI, Bergeron JJ (1994). Concentration of intracellular hepatic apolipoprotein E in Golgi apparatus saccular distensions and endosomes. J Cell Biol 127, 1859–1869.

de Hoon MJ, Imoto S, Nolan J, Miyano S (2004). Open source clustering software. Bioinformatics 20, 1453–1454.

Dmitrieff S, Sens P (2013). Transient domain formation in membrane-bound organelles undergoing maturation. Phys Rev E Stat Nonlin Soft Matter Phys 88, 062704.

Dominguez M, Dejgaard K, Fullekrug J, Dahan S, Fazel A, Paccaud JP, Thomas DY, Bergeron JJ, Nilsson T (1998). gp25L/emp24/p24 protein family members of the *cis*-Golgi network bind both COP I and II coatomer. J Cell Biol 140, 751–765.

Dym M, Clermont Y (1970). Role of spermatogonia in the repair of the seminiferous epithelium following X-irradiation of the rat testis. Am J Anat 128, 265–282.

Dym M, Fawcett DW (1970). The blood-testis barrier in the rat and the physiological compartmentation of the seminiferous epithelium. Biol Reprod 3, 308–326.

Eddy EM (1999). Role of heat shock protein HSP70–2 in spermatogenesis. Rev Reprod 4, 23–30.

Eisen MB, Spellman PT, Brown PO, Botstein D (1998). Cluster analysis and display of genome-wide expression patterns. Proc Natl Acad Sci USA 95, 14863–14868.

Emr S, Glick BS, Linstedt AD, Lippincott-Schwartz J, Luini A, Malhotra V, Marsh BJ, Nakano A, Pfeffer SR, Rabouille C, *et al.* (2009). Journeys through the Golgi–taking stock in a new era. J Cell Biol 187, 449–453.

Farquhar MG, Palade GE (1998). The Golgi apparatus: 100 years of progress and controversy. Trends Cell Biol 8, 2–10.

Fujiwara Y, Ogonuki N, Inoue K, Ogura A, Handel MA, Noguchi J, Kunieda T (2013). t-SNARE syntaxin2 (STX2) is implicated in intracellular transport of sulfoglycolipids during meiotic prophase in mouse spermatogenesis. Biol Reprod 88, 141.

Fukuda MN, Akama TO (2002). In vivo role of alpha-mannosidase IIx: ineffective spermatogenesis resulting from targeted disruption of the Man2a2 in the mouse. Biochim Biophys Acta 1573, 382–387.

Fukuda MN, Akama TO (2003a). The in vivo role of alpha-mannosidase IIx and its role in processing of N-glycans in spermatogenesis. Cell Mol Life Sci 60, 1351–1355.

Fukuda MN, Akama TO (2003b). The role of N-glycans in spermatogenesis. Cytogenet Genome Res 103, 302–306.

Gannon J, Bergeron JJ, Nilsson T (2011). Golgi and related vesicle proteomics: simplify to identify. Cold Spring Harb Perspect Biol 3, a005421.

Gilchrist A, Au CE, Hiding J, Bell AW, Fernandez-Rodriguez J, Lesimple S, Nagaya H, Roy L, Gosline SJ, Hallett M, *et al.* (2006). Quantitative proteomics analysis of the secretory pathway. Cell 127, 1265–1281.

Greenbaum MP, Iwamori N, Agno JE, Matzuk MM (2009). Mouse TEX14 is required for embryonic germ cell intercellular bridges but not female fertility. Biol Reprod 80, 449–457.

Griffiths G, Warren G, Stuhlfauth I, Jockusch BM (1981). The role of clathrin-coated vesicles in acrosome formation. Eur J Cell Biol 26, 52–60.

Hatakeyama H, Kanzaki M (2011). Molecular basis of insulin-responsive GLUT4 trafficking systems revealed by single molecule imaging. Traffic 12, 1805–1820.

Hecht NB (1990). Regulation of "haploid expressed genes" in male germ cells. J Reprod Fertil 88, 679–693.

Hermo L, Clermont Y, Rambourg A (1979). Endoplasmic reticulum-Golgi apparatus relationships in the rat spermatid. Anat Rec 193, 243–255.

Hermo L, Dworkin J, Oko R (1988). Role of epithelial clear cells of the rat epididymis in the disposal of the contents of cytoplasmic droplets detached from spermatozoa. Am J Anat 183, 107–124.

Hermo L, Pelletier RM, Cyr DG, Smith CE (2010a). Surfing the wave, cycle, life history, and genes/proteins expressed by testicular germ cells. Part 2: changes in spermatid organelles associated with development of spermatozoa. Microsc Res Tech 73, 279–319.

Hermo L, Pelletier RM, Cyr DG, Smith CE (2010b). Surfing the wave, cycle, life history, and genes/proteins expressed by testicular germ cells. Part 3: developmental changes in spermatid flagellum and cytoplasmic droplet and interaction of sperm with the zona pellucida and egg plasma membrane. Microsc Res Tech 73, 320–363.

Hermo L, Rambourg A, Clermont Y (1980). Three-dimensional architecture of the cortical region of the Golgi apparatus in rat spermatids. Am J Anat 157, 357–373.
Hermo L, Schellenberg M, Liu LY, Dayanandan B, Zhang T, Mandato CA, Smith CE (2008). Membrane domain specificity in the spatial distribution of aquaporins 5, 7, 9, and 11 in efferent ducts and epididymis of rats. J Histochem Cytochem 56, 1121–1135.
Hoskins DD, Brandt H, Acott TS (1978). Initiation of sperm motility in the mammalian epididymis. Fed Proc 37, 2534–2542.
Huang G, Buckler-Pena D, Nauta T, Singh M, Asmar A, Shi J, Kim JY, Kandror KV (2013). Insulin responsiveness of glucose transporter 4 in 3T3-L1 cells depends on the presence of sortilin. Mol Biol Cell 24, 3115–3122.
Huang HH, Stanley P (2010). A testis-specific regulator of complex and hybrid N-glycan synthesis. J Cell Biol 190, 893–910.
Igdoura SA, Herscovics A, Lal A, Moremen KW, Morales CR, Hermo L (1999). Alpha-mannosidases involved in N-glycan processing show cell specificity and distinct subcompartmentalization within the Golgi apparatus of cells in the testis and epididymis. Eur J Cell Biol 78, 441–452.
Jerome-Majewska LA, Achkar T, Luo L, Lupu F, Lacy E (2010). The trafficking protein Tmed2/p24beta(1) is required for morphogenesis of the mouse embryo and placenta. Dev Biol 341, 154–166.
Kearney R, Blondeau F, McPherson P, Bell A, Servant F, Drapeau M, de Grandpre S, Bergeron JJM (2005). Elimination of redundant protein identifications in high throughput proteomics. Conf Proc IEEE Eng Med Biol Soc 5, 4803–4806.
Klumperman J (2011). Architecture of the mammalian Golgi. Cold Spring Harb Perspect Biol 3, a005181.
Kremer JR, Mastronarde DN, McIntosh JR (1996). Computer visualization of three-dimensional image data using IMOD. J Struct Biol 116, 71–76.
Lavieu G, Dunlop MH, Lerich A, Zheng H, Bottanelli F, Rothman JE (2014). The Golgi ribbon structure facilitates anterograde transport of large cargoes. Mol Biol Cell 25, 3028–3036.
Lavieu G, Zheng H, Rothman JE (2013). Stapled Golgi cisternae remain in place as cargo passes through the stack. Elife 2, e00558.
Leblond CP, Clermont Y (1952). Definition of the stages of the cycle of the seminiferous epithelium in the rat. Ann NY Acad Sci 55, 548–573.
Lerer-Goldshtein T, Bel S, Shpungin S, Pery E, Motro B, Goldstein RS, Bar-Sheshet SI, Breitbart H, Nir U (2010). TMF/ARA160: a key regulator of sperm development. Dev Biol 348, 12–21.
Liaunardy-Jopeace A, Bryant CE, Gay NJ (2014). The COP II adaptor protein TMED7 is required to initiate and mediate the delivery of TLR4 to the plasma membrane. Sci Signal 29, ra70.
Linder B, Bammer S, Heinlein UA (1995). Delayed translation and posttranslational processing of cyritestin, an integral transmembrane protein of the mouse acrosome. Exp Cell Res 221, 66–72.
Liu H, Sadygov RG, Yates JR 3rd (2004). A model for random sampling and estimation of relative protein abundance in shotgun proteomics. Anal Chem 76, 4193–4201.
Loveland KL, Hogarth C, Szczepny A, Prabhu SM, Jans DA (2006). Expression of nuclear transport importins beta 1 and beta 3 is regulated during rodent spermatogenesis. Biol Reprod 74, 67–74.
Mamelak D, Lingwood C (2001). The ATPase domain of hsp70 possesses a unique binding specificity for 3′-sulfogalactolipids. J Biol Chem 276, 449–456.
Miller VJ, Sharma P, Kudlyk TA, Frost L, Rofe AP, Watson IJ, Duden R, Lowe M, Lupashin VV, Ungar D (2013). Molecular insights into vesicle tethering at the Golgi by the conserved oligomeric Golgi (COG) complex and the golgin TATA element modulatory factor (TMF). J Biol Chem 288, 4229–4240.
Moreno RD, Ramalho-Santos J, Chan EK, Wessel GM, Schatten G (2000a). The Golgi apparatus segregates from the lysosomal/acrosomal vesicle during rhesus spermiogenesis: structural alterations. Dev Biol 219, 334–349.
Moreno RD, Ramalho-Santos J, Sutovsky P, Chan EK, Schatten G (2000b). Vesicular traffic and Golgi apparatus dynamics during mammalian spermatogenesis: implications for acrosome architecture. Biol Reprod 63, 89–98.
Nilsson T, Hoe MH, Slusarewicz P, Rabouille C, Watson R, Hunte F, Watzele G, Berger EG, Warren G (1994). Kin recognition between medial Golgi enzymes in HeLa cells. EMBO J 13, 562–574.
O'Brien DA, Welch JE, Fulcher KD, Eddy EM (1994). Expression of mannose 6-phosphate receptor messenger ribonucleic acids in mouse spermatogenic and Sertoli cells. Biol Reprod 50, 429–435.
Oko R, Hermo L, Chan PT, Fazel A, Bergeron JJ (1993). The cytoplasmic droplet of rat epididymal spermatozoa contains saccular elements with Golgi characteristics. J Cell Biol 123, 809–821.
Ou WJ, Cameron PH, Thomas DY, Bergeron JJ (1993). Association of folding intermediates of glycoproteins with calnexin during protein maturation. Nature 364, 771–776.
Pan S, Cheng X, Sifers RN (2013). Golgi-situated endoplasmic reticulum alpha-1, 2-mannosidase contributes to the retrieval of ERAD substrates through a direct interaction with gamma-COP. Mol Biol Cell 24, 1111–1121.
Patterson GH, Hirschberg K, Polishchuk RS, Gerlich D, Phair RD, Lippincott-Schwartz J (2008). Transport through the Golgi apparatus by rapid partitioning within a two-phase membrane system. Cell 133, 1055–1067.
Pettersen EF, Goddard TD, Huang CC, Couch GS, Greenblatt DM, Meng EC, Ferrin TE (2004). UCSF Chimera–a visualization system for exploratory research and analysis. J Comput Chem 25, 1605–1612.
Ramalho-Santos J, Moreno RD, Wessel GM, Chan EK, Schatten G (2001). Membrane trafficking machinery components associated with the mammalian acrosome during spermiogenesis. Exp Cell Res 267, 45–60.
Rambourg A, Clermont Y, Hermo L (1979). Three-dimensional architecture of the Golgi apparatus in Sertoli cells of the rat. Am J Anat 154, 455–476.
Reiterer V, Nyfeler B, Hauri HP (2010). Role of the lectin VIP36 in post-ER quality control of human α1-antitrypsin. Traffic 11, 1044–1055.
Rizzo R, Parashuraman S, Mirabelli P, Puri C, Lucocq J, Luini A (2013). The dynamics of engineered resident proteins in the mammalian Golgi complex relies on cisternal maturation. J Cell Biol 201, 1027–1036.
Rosario MO, Perkins SL, O'Brien DA, Allen RL, Eddy EM (1992). Identification of the gene for the developmentally expressed 70 kDa heat-shock protein (P70) of mouse spermatogenic cells. Dev Biol 150, 1–11.
Schimmoller F, Diaz E, Muhlbauer B, Pfeffer SR (1998). Characterization of a 76 kDa endosomal, multispanning membrane protein that is highly conserved throughout evolution. Gene 216, 311–318.
Seemann J, Jokitalo E, Pypaert M, Warren G (2000). Matrix proteins can generate the higher order architecture of the Golgi apparatus. Nature 407, 1022–1026.
Smirle J, Au CE, Jain M, Dejgaard K, Nilsson T, Bergeron J (2013). Cell biology of the endoplasmic reticulum and the Golgi apparatus through proteomics. Cold Spring Harb Perspect Biol 5, a015073.
Strating JR, Martens GJ (2009). The p24 family and selective transport processes at the ER-Golgi interface. Biol Cell 101, 495–509.
Suarez-Quian CA, An Q, Jelesoff N, Dym M (1991). The Golgi apparatus of rat pachytene spermatocytes during spermatogenesis. Anat Rec 229, 16–26.
Susi FR, Leblond CP, Clermont Y (1971). Changes in the Golgi apparatus during spermiogenesis in the rat. Am J Anat 130, 251–267.
Tang XM, Lalli MF, Clermont Y (1982). A cytochemical study of the Golgi apparatus of the spermatid during spermiogenesis in the rat. Am J Anat 163, 283–294.
Thorne-Tjomsland G, Clermont Y, Hermo L (1988). Contribution of the Golgi apparatus components to the formation of the acrosomic system and chromatoid body in rat spermatids. Anat Rec 221, 591–598.
Thorne-Tjomsland G, Clermont Y, Tang XM (1991). Glucose-6-phosphatase activity of endoplasmic reticulum and Golgi apparatus in spermatocytes and spermatids of the rat: an electron microscopic cytochemical study. Biol Cell 17, 14–33.
Tokuhiro K, Ikawa M, Benham AM, Okabe M (2012). Protein disulfide isomerase homolog PDILT is required for quality control of sperm membrane protein ADAM3 and male fertility [corrected]. Proc Natl Acad Sci USA 109, 3850–3855.
Tulkens P, Trouet A (1978). The uptake and intracellular accumulation of aminoglycoside antibiotics in lysosomes of cultured rat fibroblasts. Biochem Pharmacol 27, 415–424.
van Lith M, Karala AR, Bown D, Gatehouse JA, Ruddock LW, Saunders PT, Benham AM (2007). A developmentally regulated chaperone complex for the endoplasmic reticulum of male haploid germ cells. Mol Biol Cell 18, 2795–2804.
Wong M, Munro S (2014). Membrane trafficking. The specificity of vesicle traffic to the Golgi is encoded in the golgin coiled-coil proteins. Science 346, 1256898.
Yamane J, Kubo A, Nakayama K, Yuba-Kubo A, Katsuno T, Tsukita S, Tsukita S (2007). Functional involvement of TMF/ARA160 in Rab6-dependent retrograde membrane traffic. Exp Cell Res 313, 3472–3485.
Zakariyah A, Hou W, Slim R, Jerome-Majewska L (2012). TMED2/p24beta1 is expressed in all gestational stages of human placentas and in choriocarcinoma cell lines. Placenta 33, 214–219.